2014

# The Lattice Boltzmann Methods and Their Applications to Fluid Flows

Dennis Ekin Oztekin
*Lehigh University*

# The Lattice Boltzmann Methods and Their Applications to Fluid Flows

By

Dennis Oztekin

A Thesis

Presented to the Graduate and Research Committee

Of Lehigh University

In Candidacy for the Degree of

Master of Science

In

Mechanical Engineering

Lehigh University

August 2014

Copyright page

## Thesis Signature Sheet

This thesis is accepted and approved in partial fulfillment of the requirements for the

Master of Science

_____

Date Approved

_____

Dr. Eric Varley, Thesis Advisor

_____

Dr. Gary Harlow, Chairperson
Mechanical Engineering and Mechanics

## Acknowledgments

The author would like to extend his thanks to his thesis advisor, Dr Eric Varley, for his guidance. The author is thankful for to Professor Varley for teaching theoretical fluid mechanics. A thanks is extended to the doctoral candidate Saeed Almalowi for starting the Lehigh Lattice Boltzmann group. A thanks is also extended to Greg Scott for spending hours in the computer labs working alongside me. Finally the author would like thank his parents Dr. Alparslan Oztekin and Hulya A. Oztekin for their support.

## Table of contents

## List of Figures

## 1. Abstract

The history of the Lattice Boltzmann Method and its application to fluid mechanics are investigated here. Detailed formulations are provided to form a basis for the Lattice Boltzmann Method and its many variations. These variations are designed to overcome shortcomings in the standard single relaxation time Lattice Boltzmann model. Presented here are: a model that utilizes the non-equilibrium parts of the stress tensor, the Regularized Lattice Boltzmann model; a model that converts over to momentum space, the Multi-Relaxation Time Lattice Boltzmann model; and a model that corrects itself using the entropy equation, the entropic Lattice Boltzmann model. Extensions for the Lattice Boltzmann method are derived that include: external forces, multiphase flows, and thermal flows. Various types of boundary conditions are modeled using different approaches. A detailed explanation on extracting common macroscopic flow properties in physical units is provided. These extracted properties can be used to check temporal and spatial convergence. A two dimensional, nine velocity model and a three dimensional, fifteen velocity model are used to provide examples of a number of the approaches mentioned. A two dimensional and three dimensional lid-driven cavity flow is used to illustrate these methods.

## 2. Introduction

The Lattice Boltzmann Method, commonly abbreviated to LBM, is a newer numerical method that has been slowly garnering interest in the fluids community since the 90's. The method models the distribution of and changes in a density distribution function

using the Boltzmann kinetic equation. From this information the velocity profile is determined. This unique approach allows for the modeling of complex flows with, relatively, short computing times and without any filtering.

Work on the precursor to LBM, the Lattice Gas Automata Method or HPP Method, started as early as the 1970 under the supervision of Hardy, Pomeau and de Pazzis **[Hardy, 1976]**. Unlike modern LBM, HPP modeled the movements of discrete particles. Each particle was given an initial speed and a direction. The particles would follow a simple repeating process; first collision rules were applied, then transport rules were applied, finally the time step is completed and the algorithm returns to the collision step. During the collision step every node is searched for a collision, where a collision is defined as either two particles sharing a node or a particle on a boundary node. Wherever a collision is found the velocities are updated using a series of "rules," that are merely simplified cases derived from the conservation of momentum. After all collisions are resolved, transport occurs. In this step every particle is moved to the next node in the direction of its velocity. Now the time step ends and the processes repeats at the next time step. This HPP method was very appealing; however, it has a number of shortcomings. For starters, a massive number of particles have to be used to get a picture of the overall fluid motion. This on its own is not a problem because the "rules" in the collision step are so simple in the original HPP. Unfortunately, these simple original "rules" have no overall momentum loss. This means that the energy that is given to the particles by setting their initial velocities constant in the system forever. The "rules" can be modified to account for more complex momentum equations **[Frisch, 1986]**; however, this will enormously increase computational time when there are massive numbers of particles.

Furthermore, due to the fact that particles are represented discretely, HPP is enormously dependent on the number of lattice directions. The original HPP models were incapable of capturing vortices simply due to their 5 directional lattices: up, down, left, right, and stationary, lattice directions will be discussed in more detail later. By the nineties work on Lattice Gas Automata had come to nearly a halt as Lattice Boltzmann grew more popular.

The modern Lattice Boltzmann Method removes the discrete particles from the model. In their place, there is the density distribution function. The density distribution function is the number of particles with a certain velocity in a given small volume. **[Succi, 1991]** The Lattice Boltzmann governing equation, typically called the evolution equation, updates this density distribution function at every time step. Then, from the density distribution function the velocities are calculated. In most algorithms, the evolution equation is updated in two steps. In the spirit of the old Lattice Gas Automata method, the two steps are called the collision step and the streaming step. The first step, which updates the density distribution function at every node with a relaxation time and an equilibrium density distribution function, is the collision step. Following that, the density distribution function moves outward in a transport step; called the streaming step. Early research in LBM compared the solutions of flow problems obtained by LBM to solutions obtained by other methods, such as: Spectral Methods **[Martinez, 1994; Házi, 2006]**, Large Eddy Simulation, or experimental work. Once confidence in LBM grew investigators became more interested in what it was capable of. It was found that LBM could model turbulent flow in significantly short computational time without any filtering. This meant that, without having to wait months for a direct numerical

simulation, investigators could entirely capture large and small scale disturbances in chaotic flows.**[Benzi,1990]** Soon, investigators also realized that LBM was well suited to flows with multiple fluids. The basic reason that LBM can be so easily applied to problems with multiple fluids; is because there is no need to track fronts or interfaces. This is due to the way that LBM model multiple fluids. The two fluids each have their own density distribution functions which will be modified to account for some manner of interaction between the two fluids. **[Almalowi, 2014]** Multiple methods have appeared with this idea at their hearth. The first such method was developed by Rothman and Keller in 1988. **[Rothman, 1994]** This method operated by applying a coloring to the two fluids and then the interaction were modeling though the local fluxes at each point. This so called R-K model was developed even before LBM on the Lattice Gas Automata method. Some investigators adapted it to LBM **[Gunstensen, 1991]**, however the method still retains many of the problems with the exaggerated effects of numerical noise that could be seen in the Lattice Gas Automata method. Since then a more practical method was developed by Shan and Chen. **[Shan, 1993]** The idea in this method, S-C method, is to add the effects of the other fluids as a so called interactive force between the fluids which can be added directly to the equilibrium equation. This method has caught on the most due to the simplicity of its application and it computational ease. However development in this area did not stop with the S-C model. Shortly after the S-C model was introduced, Swift et al. introduced a free energy model **[Swift, 1995].** The idea here is to re-derive the equation for the equilibrium density function using a free energy function. Following his method the equilibrium function can be made to include a variety of effects include the effects of multiphase systems. Following this in the late nineties He

et al. showed that all of these methods could be derived from the Boltzmann equation from kinetic theory **[He, 2002]**. They each simply apply different simplifications and approximations the same governing equation and should; therefore, each produces the same solutions, albeit, with various levels of accuracy. He et al. also produced their own method for dealing with multiphase problems, called the He method. He also derives a new equilibrium density distribution function; however, his model relies on a second equilibrium function for pressure **[He,1999]**. In this work the S-C model will be focused on due to the ease with which it can be applied to a variety of problems.

During these early studies into the effectiveness of LBM it was documented by a number of investigators that LBM had stability issues at relatively low Reynolds numbers; relative to what can be handled by other methods **[Almalowi, 2013]**. This is because, when the flow velocity or the spatial gradient becomes too large at a single lattice some directions of the distribution function become negative. Since the distribution function cannot be negative in any direction ever, this stops the model. After this point the solution will diverge and all numbers produced will be irrelevant. Realizing this, researcher began trying a variety of modifications of LBM to improve the range over which LBM is stable. One of these ideas was to introduce multiple relaxation times into the model. This method, introduced by D'Humieres et al., transforms the right hand side of the evolution equation from velocity space to moment space by multiplying by a linear mapping. In moment space the problem has multiple equilibrium equation and multiple relaxation times **[D'Humieres, 2002]**. The simplest way to understand why this is more stable is to imagine the system of equations formed by transforming into moment space as safety nets. If any single equation begins to diverge from a stable solution the other

equations in the system should rein it back. The multi-relaxation time LBM, MRTLBM is stable for much higher Reynolds number flows then the standard LBM. From past studies, the present investigator showed that MRTLBM remains stable up to Reynolds numbers an order of magnitude higher then single relaxation time LBM **[Almalowi, in review]**. However, MRTLBM has a serious drawback, while it does its job of increasing the range of stable Reynolds numbers for a flow simulation, it also increase the computational time.

Following this ideology of changing the definition of relaxation time, the next idea for the modification of LBM was the entropic method. Here the idea is to correct the relaxation time every time step so that if the solution begins to diverge from a stable solution the corrected relaxation time should rein it in. To know what relaxation time will correct the instability an entropy function will be examined. Different researchers have proposed different ways to do this. Karlin et al. **[Karlin, 1998, 1999]** thought to use a discretized weighted form of the continuum Boltzmann entropy function. Around the same time Boghosian et al. **[Boghosian, 2001]** thought to use Tsallis entropy function. The two groups worked together to demonstrate the validity of these types of entropic LB methods [**Boghosian, 2003**]. Eventually Keating et al. **[Keating, 2007]** showed that the two methods both satisfy the Navier Stokes equation. In this paper the focus will be more on Karlin's method. The Entropic LBM has been shown to be stable up to very high speeds without the considerable computational drawback of MRTLBM **[Aidun, 2010]**.

There exists another method to improve the stability of LBM, Regularized LBM or RLBM **[Latt, 2006].** In RLBM the density distribution function on the collision side of

the evolution equation is broken into its equilibrium component and non-equilibrium component. Next using a term for the non-equilibrium stress the collision term can be brought back to a usable form. This method does not increase the stable range of LBM as drastically as ELBM or MRTLBM; however it also adds nothing to the computational time. Furthermore the present investigator showed that it can be easily combined with MRTLBM to even further increase the range of stable Reynolds numbers for a problem **[Almalowi, in review].**

## 3. Governing equations

### a) Units and Lattice Arrangements

Before the model of LBM is presented there are a few issues that should be addressed. The lattice variables, while typically retaining the same or similar notation as their real counterparts are not identical in value. As outlined by Succi **[Succi, 2001]**, the general rule is to obtain the lattice parameters using the discretization parameters $\delta_x$ and $\delta_t$ In effect $\delta_x$ is the spacing between two adjacent lattice nodes and $\delta_t$ is the time of a single time step. The lattice parameters, $\delta_x$ and $\delta_t$, are easy to control; as a result it is not uncommon to see investigators choose their time and length steps such that their lattice parameters are always one. This constraint simplifies a great deal of LBM's governing equations and is valid, because there is some flexibility in how the conversion factors between lattice parameters and real parameters are selected. However in this study it will be avoided. From the experiences of the present author, it can be said that this is simply too great a constraint. While there is a great deal of flexibility in the conversions, there

are also a number of parameters which must remain within small ranges so as to maintain stability and accuracy.

To convert between lattice parameters and real parameters the three conversion factors, L0, T0, and M0 are used **[Llewellin, 2010]**. The simplest conversion is $L0 = \frac{d_x}{\delta_x}$, where $d_x$ is simply the length of the system in physical units divided by the number of nodes along that length. Simply put, $d_x$, is the distance between to adjacent nodes in real world units. The length of the system is fixed by the geometry being studied; however because the number of nodes may be set to be as large as necessary, provided the computational power and time are available, $d_x$ can be set in any way. The second conversion factor to determine is M0. This is the conversion from the lattice unit of mass to the real unit of mass and is defined by $\rho_{0,real} = \frac{\rho_{0,LBM} * M0}{L0^3}$. The $\rho$'s are densities in their respective units. The final conversion factor is T0, the conversion from lattice time to real time. This is defined as $T0 = \frac{d_t}{\delta_t}$. Like in the case of the spatial dimension, $d_t$is in real world units. Here it is the time between two consecutive time steps. Unlike $d_x$, $d_t$ cannot be chosen arbitrarily. It is completely constrained by the physical parameters of the problem. This makes determining T0 less straightforward then its spatial counterpart. To determine T0 first some of the parameters of the problem must be fixed. To determine T0, one starts by taking advantage of the fact that Reynolds number, $Re = \frac{U*L}{\nu}$ where U is the magnitude of the velocity, L is the characteristic length, and $\nu$ is the kinematic viscosity; is a non-dimensional term and therefore its value should be the same regardless of whether it was calculated in lattice units or real units. This yields, $\frac{\frac{\delta_x}{\delta_t} * \delta_x}{\nu_{LBM}} = \frac{\frac{d_x}{d_t} * d_x}{\nu_{REAL}}$, typically this equation

is solved for $d_t$. In the case where the kinematic viscosity is known in real units, as is usually the case in fluid mechanics; the next step becomes determining the kinematic viscosity in lattice units. Fortunately, viscosity in lattice units can be derived from the relaxation time of the problem, a parameter which comes from the discretization of the Boltzmann equation, discussed later. This relationship is $\nu_{LBM} = \left(\tau - \frac{1}{2}\right)\frac{{\delta_x}^2}{3*\delta_t}$; the relaxation time $\tau$ will also be discussed later. For the rest of this work all units, unless stated otherwise, can be assumed to be in lattice units.

Also worth noting before continuing is the peculiar behavior of density, $\rho_0$. In the present investigation, and in all LBM investigations in fluid mechanics, what is being studied is an incompressible fluid. This, of course, means that $\rho(\boldsymbol{x}, t) = \rho_0$. However, in LBM the density at each node is capable of changing, in fact this change is what drive the flow. This fluctuating density at each node is "local" density, $\rho$. The local density is typically treated as the density of a compressible gas; thereby, it can be related to pressure, $P$, by an equation of state. A typical example from the ideal gas equation is $P = \rho * c_s$; $c_s$is the lattice speed of sound, defined to be $c_s = \frac{\delta_x}{\delta_t\sqrt{3}}$.

A description of the lattice structure is also necessary before continuing. In LBM research it is common to refer to the lattice being studied as DnQl, where n and l are numbers. In this shorthand, the n is the number of spatial dimensions and the l is the number of lattice directions at each node. Unless it says otherwise all of the present study was done using D2Q9, which is depicted in Figure 1.

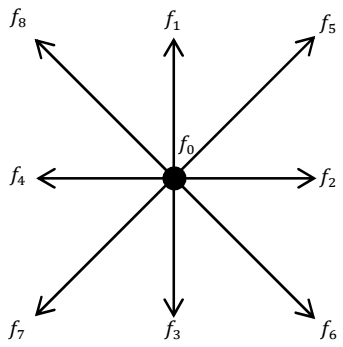


Figure 1 D2Q9 arrangement for lattice inside the flow domain

Once the lattice structure is determined the lattice velocity, $\boldsymbol{e}_k$, can be represented. The lattice velocity is the lattice speed in lattice direction $0 \leq \mathrm{k} \leq l$. Here the lattice speed is simply $c = \frac{\delta_x}{\delta_t}$. With this, the lattice velocity in D2Q9 becomes

$$\boldsymbol{e}_k = \begin{pmatrix} 0 & 0 & c & 0 & -c & c & c & -c & -c \\ 0 & c & 0 & -c & 0 & c & -c & -c & c \end{pmatrix} \tag{1}$$

Also with the lattice geometry set we can determine the weighting function. The weighting function can be determined from the low Mach expansion of an energy Maxwellian. This has already been done for any reasonable lattice geometry. In the case of D2Q9, the weighting function becomes:

$$w_k = (16/36 \quad 4/36 \quad 4/36 \quad 4/36 \quad 4/36 \quad 1/36 \quad 1/36 \quad 1/36 \quad 1/36) \tag{2}$$

It is easiest to think of this as the probability of a particle of follow each of the possible lattice paths when left to its own devices. This probability explanation is reinforced by the fact that the sum of the weighting function in all directions must be one. For greater detail see Succi **[Succi, 2001]**.

**b) Single Relaxation Time LBM**

The Boltzmann relation which all of LBM research is based on is

$$\frac{\partial f}{\partial t} + \boldsymbol{\zeta} \cdot \nabla f + \frac{\boldsymbol{F}}{m_p}\frac{\partial f}{\partial \boldsymbol{\zeta}} = \left(\frac{\partial f}{\partial t}\right)_{collision} \tag{3}$$

In equation (3) $\boldsymbol{v}$ is the particle velocity, $\boldsymbol{F}$ is the term of body forces, and $m_p$ is the particle mass. $f$ is the density distribution function mentioned earlier. To give it a more precise definition it is: for some position and some time, the number of particles per volume with a velocity between $\boldsymbol{\zeta}$ and $\boldsymbol{\zeta}$ + d $\boldsymbol{\zeta}$. Expressing this mathematically,

$$\rho = \int f d\boldsymbol{\zeta} \tag{4}$$

This relation, which defines $f$, is called the first moment of $f$. The second moment of $f$ is will also be necessary later, when recovering the conservation of momentum from the Boltzmann equation. This is

$$\rho \boldsymbol{u} = \int \boldsymbol{\zeta} f d\boldsymbol{\zeta} \tag{5}$$

It should be stressed here that $\boldsymbol{\zeta}$ is the particle velocity, this is a microscopic quantity, as opposed to **u**, that is the bulk fluid velocity. This particle velocity only has meaning when discussing the theory in its general continuous form. Once these equations are discretized for a lattice geometry, this term will become the lattice velocities discussed above. Returning to the discussion of equation (3), in fluid mechanics the third term is dropped. This term governs the influence of external forces; however, in fluid mechanics the external forces felt by the fluids are simple enough to model with more straightforward methods. As a result, in our study and in most fluids studies this term is dropped. This is not true of every field of study though; in plasma physics, for example, the inter-particle

electromagnetic forces must be considered and this term is usually included in the form of some Maxwell Relations. Even with the third term dropped, this form of the equation is still unusable to us; since the time rate of change of $f$ due to collisions on the right hand side is a complex nonlinear term. In the 1950s Bhatnagar et al. **[Bhatnagar,1954]** introduced the approximation:

$$\left(\frac{\partial f}{\partial t}\right)_{colision} = \frac{f^{eq} - f}{\tau} \tag{6}$$

Here $\tau$ is the lattice relaxation time; which is, in the single relaxation time method below, determined by viscosity and the lattice parameters. The Boltzmann equation with this relation, sometimes called the BGK model, is what most LBM research is based on. Here is where the equilibrium density distribution function, $f^{eq}$, enters the picture. There are a couple ways to derive an equilibrium density distribution function which satisfies the Navier Stokes equations. The most general way, as demonstrated by He **[ He,1997]** , is to begin with

$$f^{eq} = \frac{\rho}{(2\pi RT)^{n/2}} e^{\frac{(\boldsymbol{\zeta}-\boldsymbol{u})^2}{2RT}} \tag{7}$$

This claims that equilibrium state of the density distribution function is a Maxwell-Boltzmann distribution. Also, two new terms make appearances in this equation, *R* and *T*. These are the universal gas constant and the temperature, respectively. Because the single relaxation time model is isothermal, $RT = {c_s}^2 = \frac{c^2}{3}$. To bring this to a more useable form, a Taylor expansion is preformed about $\boldsymbol{u}$. This results in

$$f^{eq} = \frac{3\rho}{(2\pi c^2)^{D/2}} e^{\frac{3\boldsymbol{\zeta}^2}{2c^2}} \left(1 + \frac{6\boldsymbol{\zeta u}}{c^2} - \frac{3\boldsymbol{\zeta}^2}{c^2} + \frac{9(\boldsymbol{\zeta u})^2}{c^4}\right) \tag{8}$$

Now the model needs to be discretized into a form with *l* lattice directions. To start with the moments of $f$ are simply discretized as

$$\sum_{k=0}^{l} f_k = \rho \tag{9}$$

$$\sum_{k=0}^{l} f_k \boldsymbol{e_k} = \rho \boldsymbol{u} \tag{10}$$

To discretize the equilibrium equation, the following moment integral is considered

$$\int \boldsymbol{\zeta}^m f^{eq} d\boldsymbol{\zeta} \tag{11}$$

Where *m* is some constant between zero and three for isothermal models. Given equation (8), this can be expressed as

$$\int e^{\frac{3\boldsymbol{\zeta}^2}{2c^2}} \Psi(\boldsymbol{\zeta}) d\boldsymbol{\zeta} \tag{12}$$

Where $\Psi(\boldsymbol{\zeta})$ is some polynomial function of $\boldsymbol{\zeta}$. Utilizing the Gaussian quadrature rule, this integral can be discretized as

$$\sum_{k=0}^{l} W_k e^{\frac{3\boldsymbol{e_k}^2}{2c^2}} \Psi(\boldsymbol{e_k}) \tag{13}$$

From this equation the weighting function, $w_k$, is derived. Putting this definition back into equation (8), the commonly used equilibrium equation is reached.

$$f_{\mathrm{k}}^{\mathrm{eq}} = w_k \left\{ \rho_0 + \rho_0 \left( 3 \frac{\boldsymbol{e_k} \cdot \boldsymbol{u}}{c^2} + \frac{9}{2} \frac{(\boldsymbol{e_k} \cdot \boldsymbol{u})^2}{c^4} - \frac{3}{2} \frac{|\boldsymbol{u}|^2}{c^2} \right) \right\} \tag{14}$$

Kinetic theory shows us that the conservation of mass and momentum are up held by equations (4) and (5). **[He,1997]** With this derivation of the equilibrium density distribution, it is being forced to satisfy the conservation laws. To check, equation (14) can be put into equations (9) and (10) for a D2Q9 lattice arrangement. Equation 9 yields

$$0 = \sum_{k=0}^{l} w_k \left( 3\frac{\boldsymbol{e}_k \cdot \boldsymbol{u}}{c^2} + \frac{9}{2}\frac{(\boldsymbol{e}_k \cdot \boldsymbol{u})^2}{c^4} - \frac{3}{2}\frac{|\boldsymbol{u}|^2}{c^2} \right) \tag{15}$$

Putting in the weighting function demonstrated at equation (2) this becomes

$$0 = -\frac{2}{3}\frac{|\boldsymbol{u}|^2}{c^2} + \sum_{k=1}^{4} \left( \frac{\boldsymbol{e}_k \cdot \boldsymbol{u}}{3c^2} + \frac{(\boldsymbol{e}_k \cdot \boldsymbol{u})^2}{2c^4} - \frac{|\boldsymbol{u}|^2}{6c^2} \right) + \sum_{k=5}^{8} \left( \frac{\boldsymbol{e}_k \cdot \boldsymbol{u}}{12c^2} + \frac{(\boldsymbol{e}_k \cdot \boldsymbol{u})^2}{8c^4} - \frac{|\boldsymbol{u}|^2}{24c^2} \right) \tag{16}$$

It is apparent at this point that the $\boldsymbol{e}_k \cdot \boldsymbol{u}$ will vanish over the summation and result in

$$0 = -\frac{2}{3}\frac{|\boldsymbol{u}|^2}{c^2} + \sum_{k=1}^{4} \left( \frac{(\boldsymbol{e}_k \cdot \boldsymbol{u})^2}{2c^4} - \frac{|\boldsymbol{u}|^2}{6c^2} \right) + \sum_{k=5}^{8} \left( \frac{(\boldsymbol{e}_k \cdot \boldsymbol{u})^2}{8c^4} - \frac{|\boldsymbol{u}|^2}{24c^2} \right) \tag{17}$$

Expanding the dot product this results in

$$0 = -\frac{2}{3}\frac{|\boldsymbol{u}|^2}{c^2} + \frac{|\boldsymbol{u}|^2}{3c^2} + \frac{|\boldsymbol{u}|^2}{3c^2} \tag{18}$$

This has been reduced to a tautology, showing that this choice of $f^{eq}$ satisfies the conservation of mass. A similar derivation can be shown for equation (10) to show that the conservation of momentum is held.

With all of this derived the evolution equation can be solved. This is

$$f_k(\boldsymbol{x} + \boldsymbol{e}_k \delta_t, t + \delta_t) - f_k(\boldsymbol{x}, t) = -\frac{1}{\tau}\left[ f_k(\boldsymbol{x}, t) - f_k^{eq}(\boldsymbol{x}, t) \right] \tag{19}$$

**c) Alternative Methods**

Single relaxation time LBM has a great deal of stability issues and will begin to fail even at fairly low Reynolds numbers. A great deal of the research in LBM has been in modifying the single relaxation time method to increase the range of Reynolds numbers over which the method remains stable. One simple method to improve this range is called the Regularized Lattice Boltzmann Method, RLBM. RLBM relies on the idea that all the sudden changes in LBM are happening in the part of the density distribution function which is not part of the density distribution function [**Izham, 2011**]. Therefore, if a new evolution equation were derived in a way that replaced the classical collision term with a term focused on the effects of the non-equilibrium component of the density distribution function, it would be more stable than any simple single relaxation time method.

To begin this method, first a definition for the non-equilibrium density distribution function, $f_{\mathrm{k}}^{\mathrm{neq}}$, must be established.

$$f_{\mathrm{k}}^{\mathrm{neq}}(\boldsymbol{x},t) = f_{\mathrm{k}}(\boldsymbol{x},t) - f_{\mathrm{k}}^{\mathrm{eq}}(\boldsymbol{x},t) \tag{20}$$

It would also be possible to define $f_{\mathrm{k}}^{\mathrm{neq}}$ the other way, where it equals the equilibrium term minus the total term. So long as the derivations are consistent, it won't matter. Next is introduced a stress distribution function, $\Pi_{kij}$. From the definition of stress this can be related to the density distribution function by

$$\Pi_{kij} = \sum_{k=0}^{8} \boldsymbol{e_{ki}} \boldsymbol{e_{kj}} f_k. \tag{21}$$

Then the stress distribution function, like its density counterpart, is broken into an equilibrium and non-equilibrium component.

$$\Pi_{kij}^{neq} = \Pi_{kij} - \Pi_{kij}^{eq} \tag{22}$$

This is now reworked into the form

$$\Pi_{kij}^{neq} = \Pi_{kij} - \sum_{k=0}^{8} \boldsymbol{e_{ki}} \boldsymbol{e_{kj}} f_k^{eq}. \tag{23}$$

Now, in the interest of canceling higher order contributions to our governing equation as described in Latt and Chopard [**Latt, 2006**], the following expression is found using the Chapman- Enskog expansion.

$$f_k^{neq}(\boldsymbol{x}, t) \approx f_k^{(1)} = \frac{w_k}{2c_s^4} \boldsymbol{Q}_{kij} \Pi_{ij}^{neq} \tag{24}$$

Where the tensor $\boldsymbol{Q}_{kij}$ is defined as $\boldsymbol{Q}_{kij} = \boldsymbol{e}_{ki}\boldsymbol{e}_{kj} - c_s^2 \boldsymbol{\delta}_{ij}$ and $\boldsymbol{\delta}_{ij}$ is the Kronecker delta function. Using this equation the modified evolution equation of the form is obtained

$$f_{\mathrm{k}}(\boldsymbol{x} + \boldsymbol{e}_k \delta_t, t + \delta_t) - f_{\mathrm{k}}(\boldsymbol{x}, t) = -\frac{w_k}{2\tau c_s^4} \boldsymbol{Q}_{kij} \Pi_{ij}^{neq} \tag{25}$$

RLBM does improve the range over which LBM remains stable, but not by much. This is because RLBM fails to address the main source of the instability. When the density changes by too much at a single node in a single time step, this equation will blow up and in the process destroy the method. In an attempt to better solve these stability issues past investigators **[Bouzidi,2001]** developed the Multi-Relaxation Time Lattice Boltzmann Method (MRTLBM). In the past, our group employed MRTLBM to study high Reynolds Number flows **[Almalowi, in review]**. In MRTLBM the evolution equation becomes the system of equations:

$$\boldsymbol{f}(\boldsymbol{x} + \boldsymbol{e}_k \delta_t, t + \delta_t) - \boldsymbol{f}(\boldsymbol{x}, t) = S[\boldsymbol{f}(\boldsymbol{x}, t) - \boldsymbol{f}^{eq}(\boldsymbol{x}, t)] \tag{26}$$

Where the bold face is used to denote a vector of k elements and *S* is a matrix called the collision matrix. Notice that when the collision matrix is defined as $S = \frac{1}{\tau}\boldsymbol{I}$ , where $\boldsymbol{I}$ is the identity matrix, the equation reduces to the single relaxation time LBM evolution equation. In MRTLBM the idea is to go from the velocity space where $\boldsymbol{f}$ exists to a moment space where the function $\boldsymbol{m}$ exists. Note that the vector $\boldsymbol{m}$ is made up of elements $m_b$ where the set b has the same cardinality as the set of k. Each moment $m_b$ can be found using the relation

$$m_B = \boldsymbol{\phi}_B \cdot \boldsymbol{f} \tag{27}$$

This definition clearly shows that the moments are linear combinations of $\boldsymbol{f}$. From this, basic linear theory tells us that the velocity space and the moment space must have a linear mapping

$$\boldsymbol{m} = M \cdot \boldsymbol{f} \tag{28}$$

Now choose the collision matrix in such a way that its eigenvectors are $\boldsymbol{\phi}_B$ the collision process will be naturally accomplished. Applying these relations to equation (26) will result in the MRTLBM evolution equation.

$$f_{\mathrm{k}}(\boldsymbol{x} + \boldsymbol{e}_k\delta_t, t + \delta_t) - f_{\mathrm{k}}(\boldsymbol{x}, t) = -M^{-1}\hat{S}\left[m_k(\boldsymbol{x}, t) - m_k^{eq}(\boldsymbol{x}, t)\right] \tag{29}$$

Where $\hat{S}$ is a diagonalized new collision matrix such that $\hat{S} = M \cdot S \cdot M^{-1}$. For a more detailed derivation, please refer to D'Humieres and his colleagues **[D'Humieres, 2002]**.

As described earlier, sudden changes in the density cause single relaxation time LBM to fail. This is reasonable, after all LBM as it is used in fluid mechanics was designed for use in the studying of incompressible flows; however the key mechanism which drives

the flow in LBM is changes in the local density. So long as the changes in the local density are small, LBM will capture the flow with a high degree of accuracy. If the local density variations grow large, such is the case when the velocity gradient is steep or the velocity is changing rapidly in time, the model will produce negatives and becomes incapable of recovering. The multi-relaxation time LBM solves this with a "shotgun" approach; it introduces a system of governing equations based on different physical modes for the system. If any single equation starts to blow up the other equations are there to keep the model in order. While looking at this kind of simplified description of the stability problem another possible solution comes to mind. If any information about the solution was known a head of time that information could be used to rein in the solution, thus preventing the model from blowing up. This is the idea behind the entropic LBM. Here the objective is to maintain the monotonicity of the entropy equation while maintaining the kinetic theory constraints. **[Chikatamarla, 2006]** The entropy equation chosen for this is

$$H = \sum_{k=0}^{l} f_k \ln\left(\frac{f_k}{w_k}\right) \tag{30}$$

Forcing the monotonicity introduces the non-linear equation

$$H(f_k) = H\left(f_k + \alpha * f_k^{neq}\right) \tag{31}$$

It is important to note that to stay in line with the literature $f_k^{neq}$ is defined differently than it was in RLBM, here it is

$$f_{\mathrm{k}}^{\mathrm{neq}}(\boldsymbol{x}, t) = f_{\mathrm{k}}^{\mathrm{eq}}(\boldsymbol{x}, t) - f_{\mathrm{k}}(\boldsymbol{x}, t) \tag{32}$$

From this constraint, the parameter, $\alpha$, is defined. This parameter shows up in the entropic model's modified relaxation time, $\mathrm{B} = \frac{\alpha}{2*\tau}$. With this the evolution equation becomes

$$f_k(\boldsymbol{x} + \boldsymbol{e}_k\delta_t, t + \delta_t) = \mathrm{B}\left[f_k^{eq}(\boldsymbol{x}, t) - f_k(\boldsymbol{x}, t)\right] + f_k(\boldsymbol{x}, t) \tag{33}$$

It can be seen that when $\alpha = 2$, B goes to $\frac{1}{\tau}$. This is good, since this means that single relaxation time LBM can be recovered as a special case of this entropic method. The main challenge posed by this method is that the non-linear equation (31) must be solved at every time step for every node to determine each value of alpha $\alpha$. Fortunately, from single relaxation time LBM, we know that $\alpha$ should be near two unless there are problems with stability occurring. Using the initial guess $\alpha = 2$, in other words that the flow is stable and governed by single relaxation time, we can use methods such as the Newton Raphson method. Authors have in the past claimed that, because two is such a good initial guess, only one iteration of Newton Raphson is good enough to reach sufficient accuracy. However, the present investigator prefers a slightly different method. Yasuda et al. proposed **[Yasuda, 2011, 2013]** the idea of using expansions of the Taylor Series to derive an explicit function for α. He demonstrates that when the expansion is only taken to include the first order terms, this method is equivalent to using the Newton Raphson method. While this seems uninteresting, the method can be easily extended to include higher order terms without greatly increasing the difficulty of the computation. The idea is to first break $\alpha$ into an old term and a change term.

$$\alpha = \alpha^* + \acute{\alpha} \tag{34}$$

where $\alpha^*$is the previous value of $\alpha$, initially two everywhere, and $\acute{\alpha}$ is the change in $\alpha$ this time step. Putting this expansion into the monotonicity equation (31) results in

$$H(f_k) = H\left(f_k + (\alpha^* + \acute{\alpha}) * f_k^{neq}\right) \tag{35}$$

For the sake of simplification let $f_k{}^* = f_k + \alpha^* f_k^{neq}$, which reduces the above equation to

$$H(f_k) = H\left(f_k{}^* + \acute{\alpha} f_k^{neq}\right) \tag{36}$$

Applying a Taylor expansion about the density distribution on entropy function on the right hand side produces the relation

$$H\left(f_k{}^* + \acute{\alpha} f_k^{neq}\right) = H(f_k{}^*) + \frac{d\,H(f_k{}^*)}{d\,f_k{}^*} * \left(\acute{\alpha} f_k^{neq}\right) + \frac{d^2\,H(f_k{}^*)}{d\,f_k{}^{*2}} * \frac{\left(\acute{\alpha} f_k^{neq}\right)^2}{2} + \frac{d^3\,H(f_k{}^*)}{d\,f_k{}^{*3}} * \frac{\left(\acute{\alpha} f_k^{neq}\right)^3}{6} + \cdots \tag{37}$$

Now the question is how many terms should be included. One investigator claimed in informal conversation that the entropic LBM is stable for any Reynolds number. The claim is clearly exaggerated, after all the model will fall apart when the flow becomes compressible. There is a grain of truth in the statement. With this formulation, the classical stability problem of LBM is completely avoided, if one can find the correct value of $\alpha$. However, by applying these discrete methods to solve for $\alpha$, a potential source of instability is once again being introduced into the model. This method is still superior to single relaxation time, even with this new source of instability because even if the model begins to diverge a solution for $\alpha$ will still be found. It is only when the solution diverges so far that this initial guess method is incapable of converging to a correct $\alpha$, will this method run into this sort of stability problems. This is where the

choice of the order of accuracy taken in the above equation comes into play. If the truncation of the Taylor expansion is done later the solution for alpha will be more accurate and less likely to diverge; however, the time it takes to run the program will increase as well. After all, $\alpha$ must be solved at every point in the lattice at every time step, so an increase in the computational difficulty of finding a single $\alpha$ value will drastically impact the computational time of the whole algorithm. In the present work the third order and greater terms will be truncated. With this truncation, the Taylor expansion can be substituted into equation (36).

$$H(f_k) = H(f_k{}^*) + \frac{d\,H(f_k{}^*)}{d\,f_k{}^*} * \left(\acute{\alpha} f_k^{neq}\right) + \frac{d^2\,H(f_k{}^*)}{d\,f_k{}^{*2}} * \frac{\left(\acute{\alpha} f_k^{neq}\right)^2}{2} \tag{38}$$

This equation needs to be solved for $\acute{\alpha}$. This is simply a quadratic equation in terms of $\acute{\alpha}$. To make this more apparent the following reductions are made.

$$\aleph_1 = \frac{d^2\,H(f_k{}^*)}{d\,f_k{}^{*2}} * \frac{f_k^{neq\,2}}{2} \tag{39}$$

$$\aleph_2 = \frac{d\,H(f_k{}^*)}{d\,f_k{}^*} * f_k^{neq} \tag{40}$$

$$\aleph_3 = H(f_k{}^*) - H(f_k) \tag{41}$$

Now the equation is in a clear quadratic form

$$\aleph_1 \acute{\alpha}^2 + \aleph_2 \acute{\alpha} + \aleph_3 = 0 \tag{42}$$

Equation (33) can be solved with the simple quadratic formula.

$$\acute{\alpha} = \frac{-\aleph_2 + \sqrt{\aleph_2{}^2 - 4\aleph_1\aleph_3}}{2\aleph_1} \tag{43}$$

Knowing the change in $\alpha$, $\alpha$ itself can be determined from

$$\alpha = \alpha^* + \frac{-\aleph_2 + \sqrt{\aleph_2{}^2 - 4\aleph_1\aleph_3}}{2\aleph_1} \tag{44}$$

With this equation, everything needed to solve for $\alpha$, which in turn is everything needed to conduct the next evolution step, is at hand. With the definition of $H(f_k)$ already given the following can be determined

$$\aleph_2 = \frac{d\,H(f_k{}^*)}{d\,f_k{}^*} * f_k^{neq} = \sum_{k=0}^{l} \left( f_k^{neq} + f_k^{neq} \ln \frac{f_k{}^*}{w_k} \right) \tag{45}$$

Similarly

$$\aleph_1 = \frac{d^2\,H(f_k{}^*)}{d\,f_k{}^{*2}} * \frac{\left(\acute{\alpha} f_k^{neq}\right)^2}{2} = \acute{\alpha}^2 \sum_{k=0}^{l} \left( \frac{f_k^{neq^2}}{f_k{}^*} \right) \tag{46}$$

**d) Multiphase Model**

LBM has shown itself to be very adept at modelling multiphase flows as shown by Hou et al. **[Hou,1997].** It completely avoids the hassle of interface tracking which slows down classical methods. To deal with multiple fluids simply introduce multiple density distribution functions: $f_k^i$, with $i = \{1 \dots q\}$ where q is the number of fluids in the system. Now the evolution equation becomes the system of equations:

$$f_k^i(\boldsymbol{x} + \boldsymbol{e_k}\delta_t, t + \delta_t) - f_k^i(\boldsymbol{x}, t) = -\frac{1}{\tau^i}\left[f_k^i(\boldsymbol{x}, t) - f_k^{i\,eq}(\boldsymbol{x}, t)\right] \tag{47}$$

As it is, this evolution equation is missing a key component for multiphase flows, inter-particle forces, $\boldsymbol{F}_{int}$. To add this effect into our model we used the method introduced by Shan and Chen. As was mentioned earlier:

$$\sum_k f_k^{i[0]} = \rho^i \text{ and } \sum_k f_k^{i[0]} \boldsymbol{e_k} = \rho^i \boldsymbol{u}^i \tag{48}$$

Now we also need a common velocity which can be found by what is effectively mass averaging:

$$\boldsymbol{u}^i = \frac{\sum_{i=1}^{\alpha} \frac{\rho^i \boldsymbol{u}^i}{\tau^i}}{\sum_{i=1}^{\alpha} \frac{\rho^i}{\tau^i}} \tag{49}$$

With this we can solve for an equilibrium velocity. Using this velocity in the calculations for $f_k^{i^{eq}}$ will automatically account for the inter-particle forces as demonstrated in Shan and Chen.

$$\rho^i \boldsymbol{u}^{i^{eq}} = \rho^i \boldsymbol{u}^i + \tau^i \boldsymbol{F}^i \tag{50}$$

Here $\boldsymbol{F}^i$ is the total inter-particle force on fluid *i* per unit volume, but it has been shown by Huang et al. [**Huang,2009**] that $\boldsymbol{F}^i$ can be extended to include other forces such as body forces and adhesion forces. A typical example of an $\boldsymbol{F}^i$ that includes the gravity force acting on a body and includes forces from the interactions between fluids is $\boldsymbol{F}^i = \boldsymbol{F}_{int}^i + \boldsymbol{F}_{body}^i$. The inter-particle force is calculated using:

$$\boldsymbol{F}_{int}^i(\boldsymbol{x}) = -\psi^i(\boldsymbol{x}) \sum_{x'} \sum_{\bar{\imath}=1}^{\alpha} G^{i\bar{\imath}}(\boldsymbol{x}, \boldsymbol{x}') \psi^{\bar{\imath}}(\boldsymbol{x}') \, (\boldsymbol{x}' - \boldsymbol{x}) \tag{51}$$

Since only the interactions between point x neighbors are being considered $G^{i\bar{\imath}}(\boldsymbol{x}, \boldsymbol{x}')$ can be written as:

$$G^{i\bar{\imath}}(\boldsymbol{x}, \boldsymbol{x}') = \begin{cases} 0, & |\boldsymbol{x} - \boldsymbol{x}'| > c \\ g^{i\bar{\imath}}, & |\boldsymbol{x} - \boldsymbol{x}'| \leq c \end{cases} \tag{52}$$

where $\mathcal{g}^{i\bar{\imath}}$ is a constant parameter which controls the strength of the inter-particle forces. Now all that remains is to calculate the effective mass which is:

$$\psi^i = \rho_0^i \left(1 - e^{-\rho^i/\rho_0^i}\right) \tag{53}$$

$\rho_0^i$ is the constant density of fluid $i$. The gravity force is much simpler:

$$\boldsymbol{F}_{body}^i = \boldsymbol{g}\rho^i \tag{54}$$

For the sake of presentation a coloring step can be added to this method in the two fluid case. The idea is to create a function $\kappa$; which is one at a node entirely dominated by the lighter fluid, negative one at a node entirely dominated by the heavier fluid, and somewhere between one and negative one for a node which consists of both the light and heavy fluid.

$$\kappa = \frac{\rho^{light} - \rho^{heavy}}{\rho^{light} + \rho^{heavy}} \tag{55}$$

At any given instant this coloring function can be contour plotted to produce an image showing where each fluid is

**e) Thermal Model**

Similar to how one can introduce another distribution function to track a second fluid, it is possible to introduce another distribution function to track the temperature. Here, instead of tracking a density distribution function, what is being introduced is a kinetic energy distribution function, $h_i$. From kinetic theory, it is known that kinetic energy can be related to temperature by

$$\frac{\rho DRT}{2} = \sum_{i=0}^{k} h_i \tag{56}$$

This comes from discretizing the third moment of $f$, not shown earlier. Here $D$ is the number of dimensions involved in the model. $R$ is the universal gas constant and $T$ is temperature **[Liu, 2010]**. Once this relationship established the motivation for tracking the kinetic energy, investigators introduced an evolution equation solely for tracking the kinetic energy distribution.

$$h_k(\boldsymbol{x} + \boldsymbol{e}_k\delta_t, t + \delta_t) - h_k(\boldsymbol{x}, t) = -\frac{1}{\tau_h}\left[h_k(\boldsymbol{x}, t) - h_k^{eq}(\boldsymbol{x}, t)\right] \tag{57}$$

The key differences between this and the normal evolution equation are the relaxation time $\tau_h$ and the equilibrium distribution $h_k^{eq}$. While both perform the same function and have similar meaning, their derivations and exact values are different. The energy relaxation time, $\tau_h$, is no longer based on the viscosity of the fluid. Rather it is based on the thermal diffusion rate. This relation goes with

$$\chi_{LBM} = \left(\tau_h - \frac{1}{2}\right)\frac{{\delta_x}^2}{3\delta_t} \tag{58}$$

where $\chi_{LBM}$ is the thermal diffusivity in lattice units. As an interesting aside, note that the Prandtl Number can be calculated though

$$Pr = \frac{\upsilon}{\chi} = \frac{\upsilon_{LBM}}{\chi_{LBM}} = \frac{\left(\tau - \frac{1}{2}\right)\frac{{\delta_x}^2}{3\delta_t}}{\left(\tau_h - \frac{1}{2}\right)\frac{{\delta_x}^2}{3\delta_t}} = \frac{\tau}{\tau_h} \tag{59}$$

This relationship can be used to fix thermal lattice units and derive the energy relaxation time **[He, 2010]**. The other term which differs between the thermal model and standard

LBM is the equilibrium equation. To derive the energy equilibrium distribution the Boltzmann energy equation is used

$$h_k^{eq} = \frac{{e_k}^2}{2} f_k^{eq} \tag{60}$$

Finally, a forcing term is typically added to force gravity into the model. After all, a large class of problems studied by researches in the field of heat and mass transfer are free convection problems. It was shown by Mohamad et al. **[Mohamad, 2010]** that the same method used by Shan and Chen to include the inter-particle force can be used to include only the gravitational force for the purposes of modeling natural convection.

**f) Boundary Conditions**

The boundary conditions have always been a prominent problem in LBM. Any lattice direction coming out from the boundary is immediately an unknown, after all it is impossible to stream fluid to the node from a lattice direction outside of the boundary. A great deal of research has been done on finding solutions to these unknown directions in the distribution function. For periodic boundaries, typically used to imitate an infinite domain, there exists a simple solution. The lattices on either side of the infinite boundary are treated to be the same lattice. For all intensive purposes, what this does is set the unknown values of the distribution function equal to the known values of the distribution function on the other side of the periodic boundary. Another type of boundary which has been well addressed in the past was the case of a boundary which is no slip, no penetration, straight, and falls entirely on lattice nodes. Common examples of this type of boundary include: the walls in a channel flow, the wall of some sort of stationary

obstruction in the flow, the walls of a cavity in which there is flow. The earliest boundary condition devised for this problem is the bounce back boundary condition. The unknown directions in the bounce back method are set equal to the directions directly opposite to them, the ones which would be streaming into the wall. Doing this is a simple and brute way to force mass conservation; it is impossible to lose any mass if all the mass that reaches the wall is just reflecting. There are a number of problems with this brute method. For one, there is no obvious way to extend this method to include affects such as a moving boundary or injection. Second, this method very much needs the boundary to fall directly on the nodes. Finally, this method is a full order of accuracy lower than the base single relaxation LBM model. For all these reasons a number of alternative methods were developed. One improvement to this basic bounce back is the mass and momentum conserving bounce back developed by Zou et al **[Zou, 1997].** Zou's method begins by identifying all the unknowns on the boundary and all the equations. What is given is: the three constraint equations from kinetic theory; the directions of the density distribution function going into the wall; the directions of the density distribution function along the wall, the actually given boundary condition (ie. density, pressure, or velocity ); and the equilibrium equations. For a D2Q9 lattice, the unknowns are density, 2 speeds, and the three directions of the density distribution function coming out of the boundary. Let us call these three directions: diagonal left, L; diagonal right, R; and normal, N. Once these equations and unknowns are written out, it becomes apparent that another equation is needed to close this set. To close these equations, Zou introduces the assumption that the non-equilibrium part of the normal direction is reflected from the wall. This is a far more flexible assumption then ordinary bounce back. It turns out that this derivation has the

same order of accuracy as single relaxation time LBM and thus the present investigator prefers to use it. Furthermore, because the derivation made no assumptions about the velocity on the boundary, this boundary condition can be used in a variety of interesting problems such as boundary driven flows, like lid driven cavities or Couette flows and injection problems, such as flow near a membrane. This method still does not address the problem of boundaries which do not lie directly on nodes. This is a fairly common occurrence when boundaries do not intersect at perfect ninety degree angles. It also is a problem that must be addressed before even considering the study of curved boundaries. The idea is to find the location of the boundary compared to the nearest lattice inside and the nearest lattice outside the boundary. Using these distances a modified evolution equation can be derived that satisfies the boundary conditions [**Mei, 2000]**. This method has a drawback, Bao et al. reports, that this method causes mass leakage in the system **[Bao, 2008]**. The present investigation has limited itself to boundaries that lie directly on the lattice nodes, so this has not been an issue. In future work, where curved boundaries may be studied, this will have to be considered.

These boundary conditions can be extended to all of the above mentioned methods in LBM, with the exception of the Entropic LBM. All of the boundary conditions treatments discussed here only concern themselves with the lattice direction that are point out from the wall. This makes sense, since in the most methods the directions coming out of the wall are the direction that stream into your fluid. Therefore, these directions are the ones that actually effect the computational domain. Unfortunately, in the entropic method, $\alpha$ is a function of the density distribution function summed over all its directions. Using any of the aforementioned boundary methods would produce an irrelevant $\alpha$. This, in turn,

would destroy the model in the next computational step. A solution to this was presented by Karlin's group **[Chikatamarla, 2013]**. The idea of this method is to use the non-equilibrium bounce back assumption mentioned in the mass and momentum conserving boundary method discussed above. Here, the difference is, the non-equilibrium bounce back is applied to every lattice direction coming out of the wall. These equations are then substituted into the entropic method's evolution equation to obtain a modified boundary conditions evolution equation. This method of treating the boundary both accurately streams the distribution function back into the fluid and derives the other directions of the density distribution function in a way that forces the boundary conditions to be satisfied.

**g) Three Dimensional Extension**

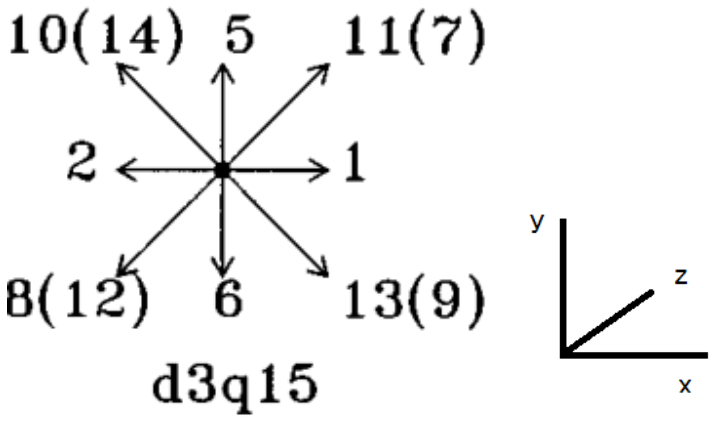


Figure 2 D3Q15 lattice arrangement. The directions in parenthesis are angled out of the paper. The directions on the diagonals not in parenthesis are angled into the paper. Not shown here is direction zero which is the node itself, direction 3 that is normal to the page facing out, and direction 4 that is normal to the page facing in.

LBM can be very easily extended to three dimensions. Here, the primary differences between the two dimensional and three dimensional models will be discussed. For all the previous methods in LBM, with the exception of the Multi-Relaxation time model, extending to three dimensions only necessitates a different weighting function and the addition of the extra dimension in the velocity vectors. In the Multi-Relaxation Time method, the number of equations must equal the number of lattice directions, so as to keep the matrix square. Because of this, a number of additional modes must be added to the system to make the method valid in three dimensions. Fortunately, none of the other LBM variations have this problem. To demonstrate the effectiveness of LBM in three dimensions the present investigator presented a three dimensional lid driven cavity, displayed later in the results section. These results were obtained using a D3Q15 Lattice arrangement shown above. As a demonstration of the simplicity of extending a two dimensional model to three dimensions, listed here are all the changes that needed to be made when extending the model from D2Q9 to D3Q15. The first, and most obvious change, was that every variable needed to be extended to account for the third dimension. Then the new velocity component was introduced, and with it a new lattice velocity was introduced. All the lattice velocities and the weighting function must be updated, as is needed whenever the lattice arrangement changes in any manner. Next the equilibrium density equation appears. This term does not change. The velocities, lattice velocities, and weighting function that it calls are all different therefore it will produce different results. Besides that, the governing equation is identical. The same holds true for the collision equation. The streaming step needs to be rewritten but this is not surprising, of course the lattice directions which the fluid is streaming over will need to change when

the lattice directions change. The boundary conditions are trickier. The periodic boundary conditions and the bounce back boundary condition are identical in three dimensions. The problem is the Zou's boundary condition. Zou's method only worked because in the D2Q9 model there happened to be the same number of equations and unknown as described above. This is not true for any other lattice arrangement. For D3Q15 this method produces six unknowns, five lattice directions and pressure, and only five equations, the non-equilibrium equation, and the four constraints equations. To get around this problem one can either adopt a method such as the one demonstrated by Maier et al **[Maier, 1996]**. Maier applies the standard bounce back condition and then redistributes the mass over the lattice directions so as to satisfy the momentum equation. The method adopted by the present investigator is to solve the kinetic mass equation and one of the kinetic momentum equations in such a way as to create a single equation that relates density to the known density distribution values and one component of velocity. As an example, derived below is a boundary conditions the case were the top boundary (z=max) is moving in one direction. This has been derived using the D3Q15 arrangement shown in figure 2.The derivation starts with equation (9) expanded

$$f_0 + f_1 + f_2 + f_3 + f_4 + f_5 + f_6 + f_7 + f_8 + f_9 + f_{10} + f_{11} + f_{12} + f_{13} + f_{14} = \rho \quad (61)$$

For the top boundary the directions 6, 8, 9, 12, and 13 are unknown. To solve these direction, the momentum equations are check. It becomes apparent when the momentum equation are expanded that only one of the momentum equation possesses these lattice directions together with the same sign and that is the y directional momentum equation.

$$f_6 + f_8 + f_9 + f_{12} + f_{13} = f_5 + f_7 + f_{10} + f_{11} + f_{14} - u_y\rho \quad (62)$$

Subtracting this from the previous equation yields

$$\rho = \frac{f_0+f_1+f_2+f_3+f_4+2*(f_5+f_7+f_{10}+f_{11}+f_{14})}{u_y-1} \tag{63}$$

With $u_y \neq 1$ this yields a relationship between the known top boundary conations and density. Next a non-equilibrium bounce back condition is introduced in the unknown lattice direction. In this example it is of the form

$$f_6 = f_5 - f_5^{eq} + f_6^{eq} \tag{64}$$

$$f_8 = f_7 - f_7^{eq} + f_8^{eq} \tag{65}$$

And so on for the other unknown lattice directions. These equation produce the right number of equations and unknown from which the following relations can be derived

$$f_6 = f_5 - \frac{2\rho u_y}{3c} \tag{66}$$

$$f_8 = f_7 - \frac{\rho}{12c}\Big(u_y + (u_x + u_z)\Big) \tag{67}$$

$$f_9 = f_{10} - \frac{\rho}{12c}\Big(u_y - (u_x + u_z)\Big) \tag{68}$$

$$f_{12} = f_{11} - \frac{\rho}{12c}\Big(u_y + (u_x + u_z)\Big) \tag{69}$$

$$f_{13} = f_{14} - \frac{\rho}{12c}\Big(u_y - (u_x + u_z)\Big) \tag{70}$$

# 4. Results and Discussions

## a) Geometry

To demonstrate some of the methods discussed above, a well lid driven cavity flow is modeled. This problem was chosen for this study due to the abundance of literature on the topic and partially due to the simplicity of the geometry involved. The lid driven cavity flow is a well-studied problem in fluid mechanics and great deal of literature can be found on this method. Even as early as the 1960's researchers were attempting to model from the full Navier Stokes equations on old IBM machines **[Burggraf, 1966]**. In the modern day may researcher continue to use the lid driven cavity as a benchmark with which to compare their results and prove their method's validity **[Botella, 1996][ Bruneau,2006].** The lid driven cavity in two dimensions consists of three no slip, no penetration boundaries and one boundary, the so called lid, which drives the flow. Depicted in figure 3 is the geometry of a two dimensional lid driven cavity flow. The three dimensional extension adds two no slip boundaries in the third dimension. This leaves five no slip no penetration boundaries and one driven lid. All the cavity flows depicted here are perfect squares and cubes, but the sake of reference the length from the side opposite the lid to the lid is defined to be the characterizing length of the problem, L. In all the cases presented here L is set to .1 meters. The Reynolds number in the base cases are all set to 300 for the purposes of comparison; however a number of results are presented at other Reynolds numbers. If the Reynolds number is set to any value other than 300 it will be labeled as such. The viscosity of the fluid is set to $10^{-6}\,\frac{m^2}{s}$, roughly the viscosity of water. In the case of the lid driven cavity flow, the maximum velocity

must occur on the top boundary. This gives the investigators a unique opportunity to fix $c_s$, the lattice speed of sound, and immediately cross reference it to the velocity of the lid. This gives certainty that the velocity in the flow domain remains well below the incompressibility limit. In these algorithms, a value $U_{max}$ is defined. This value is .15* $c_s$ and is meant to be the absolute limit on the velocity. $U_{max}$ is fixed in all of these runs as .1. Also fixed in these runs is the lattice time step, $\delta_t$, which is always set to .5 in these demonstrations. To completely determine these problems, two more variables need to be fixed. In this study the number of lattice nodes per the characteristic length, n, and the inverse of relaxation time, $\omega$, were fixed. These two variables are not the same in every run. The number of lattices was being used to control the spatial accuracy of the system and, because of the way LBM converts from real to lattice units, the temporal accuracy of the system. In the lid driven cavity flow a high temporal accuracy is unnecessary; unfortunately, because of the way LBM derives the physical time steps, maintaining a high spatial accuracy forces a high temporal accuracy. $\omega$ was used to mitigate this problem, as the physical time step is both a function of the number of lattices and the relaxation time. For the purposes of maintaining stability, in the following simulations $\omega$ is kept within the range of 1.4-1.9. Depending on what degree of spatial accuracy was needed, the number of lattices ranged between a 50x50 grid and a 500x500 grid in two dimensions. In three dimensions the only result is 50x50x50.

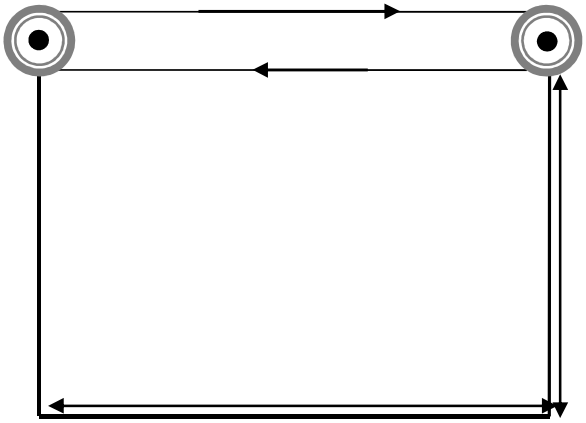

Figure 3 Geometry of the lid-driven cavity problem in two dimensions

**b) Convergence Test**

In any numerical simulation it is critical to first show that spatial and temporal convergence is achieved. In LBM spatial and temporal convergences are coupled. So when spatial convergence is demonstrated, temporal convergence is inherently proved as well. To demonstrate that the model has reached spatial and temporal convergence simulations were conducted in which all parameters were held constant, with the exception of the number of lattice nodes. These results are shown in figure 4. In figure 4 the contours of the streamlines are depicted for a 50, 100,200, 300, and 500. As observed from these images, the spatial structure of the primary vortex and the secondary vortices at the bottom are nearly the same for results obtained by the 200, 300, and 500 mesh sizes. However, the relative intensity of the secondary vortex to the primary vortex varies

with the grid sizes. For the two dimensional results presented below, grid sizes of 100 and 400 are used and for the three dimensional result, a grid size of 50 is used.

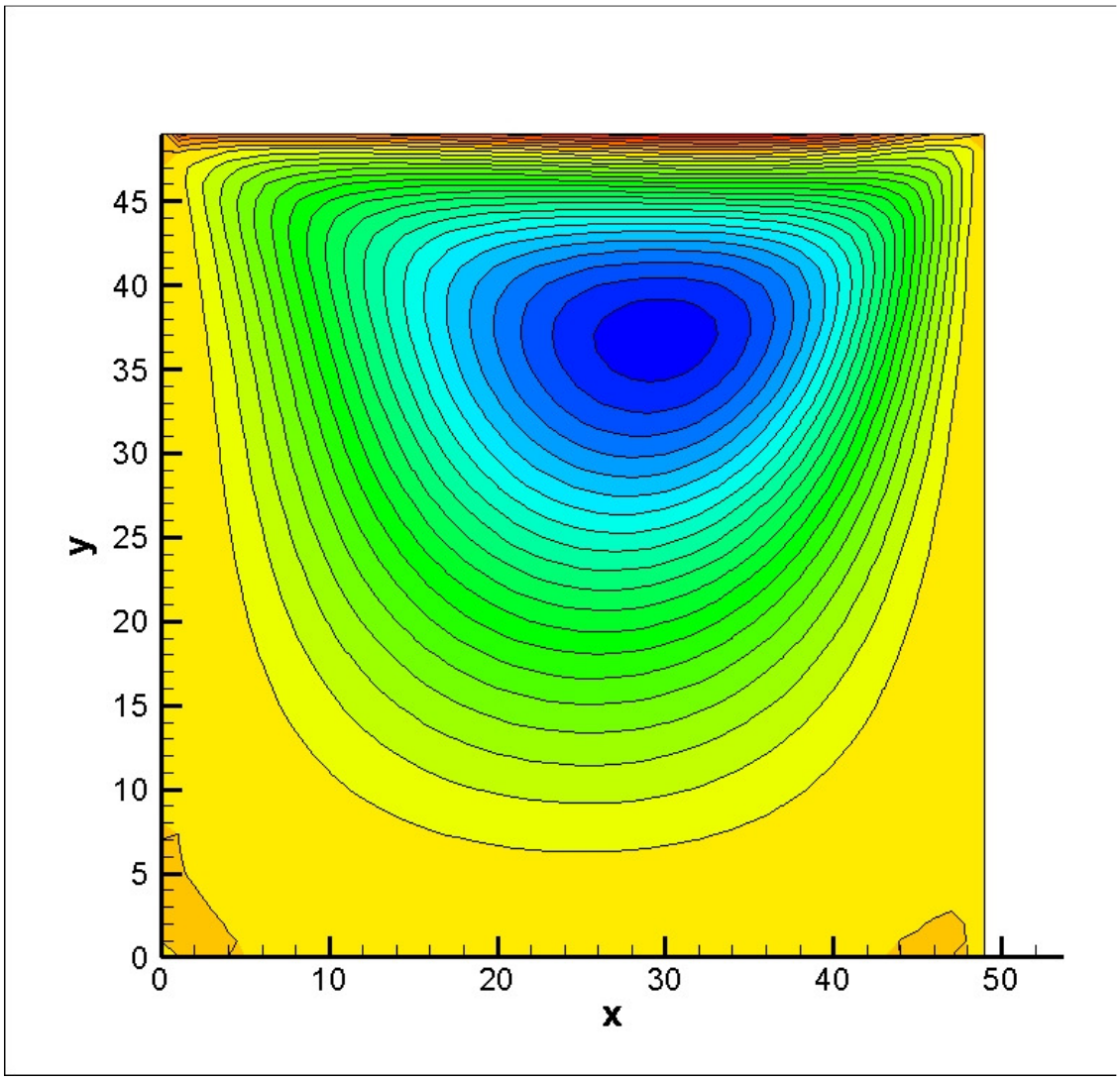


a) 50x50

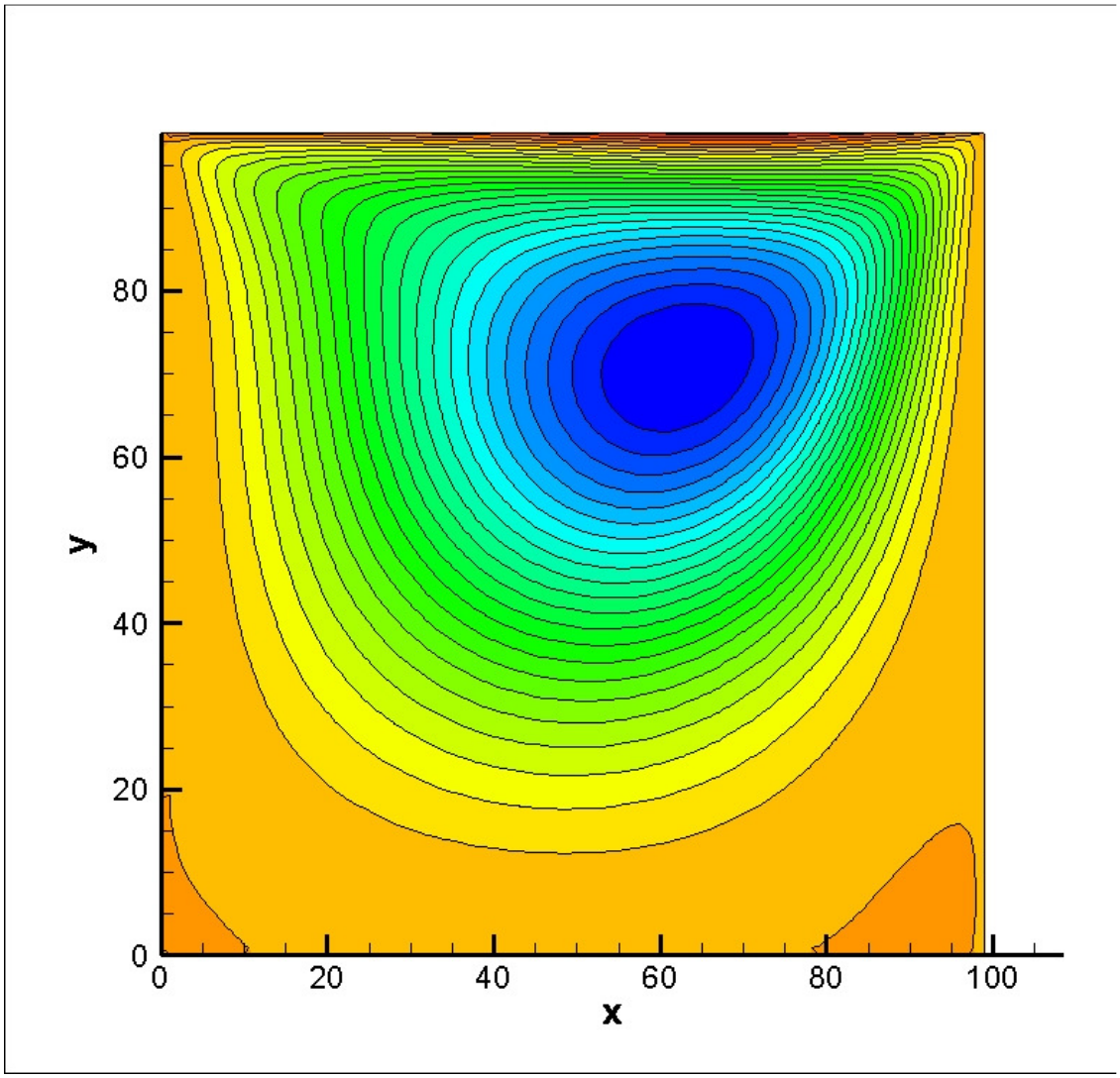


b) 100x100

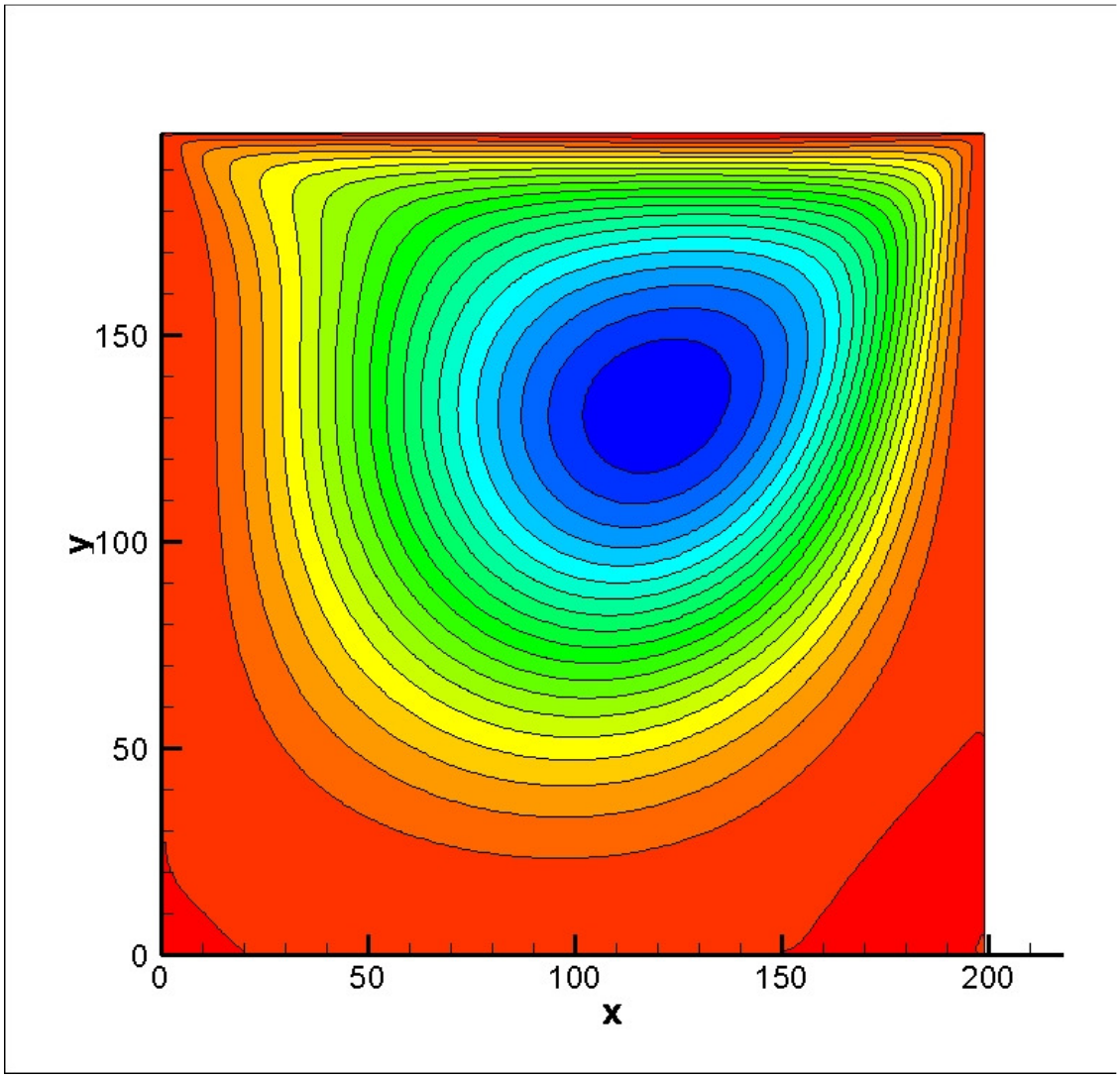


c) 200x200

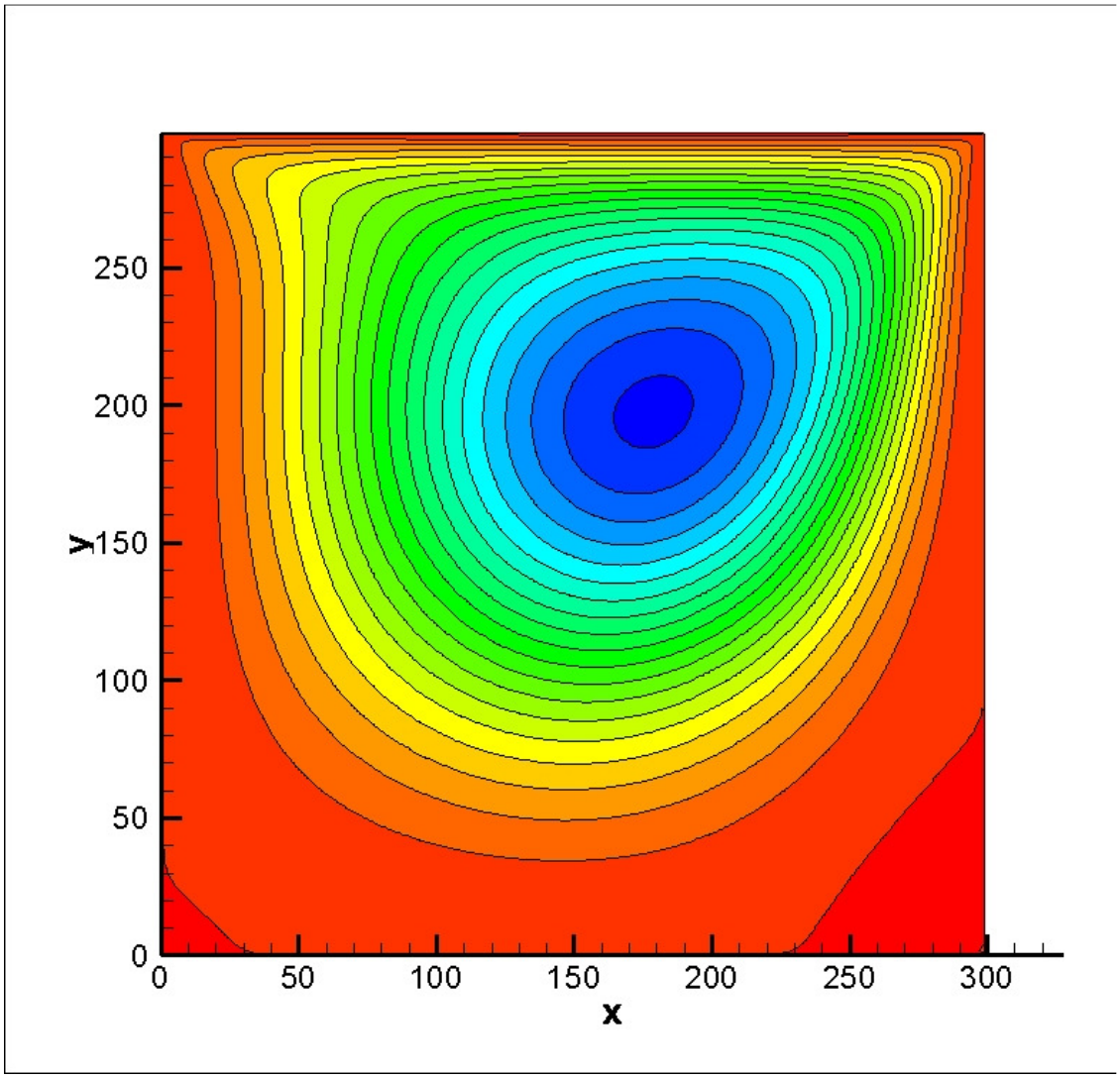


d) 300x300

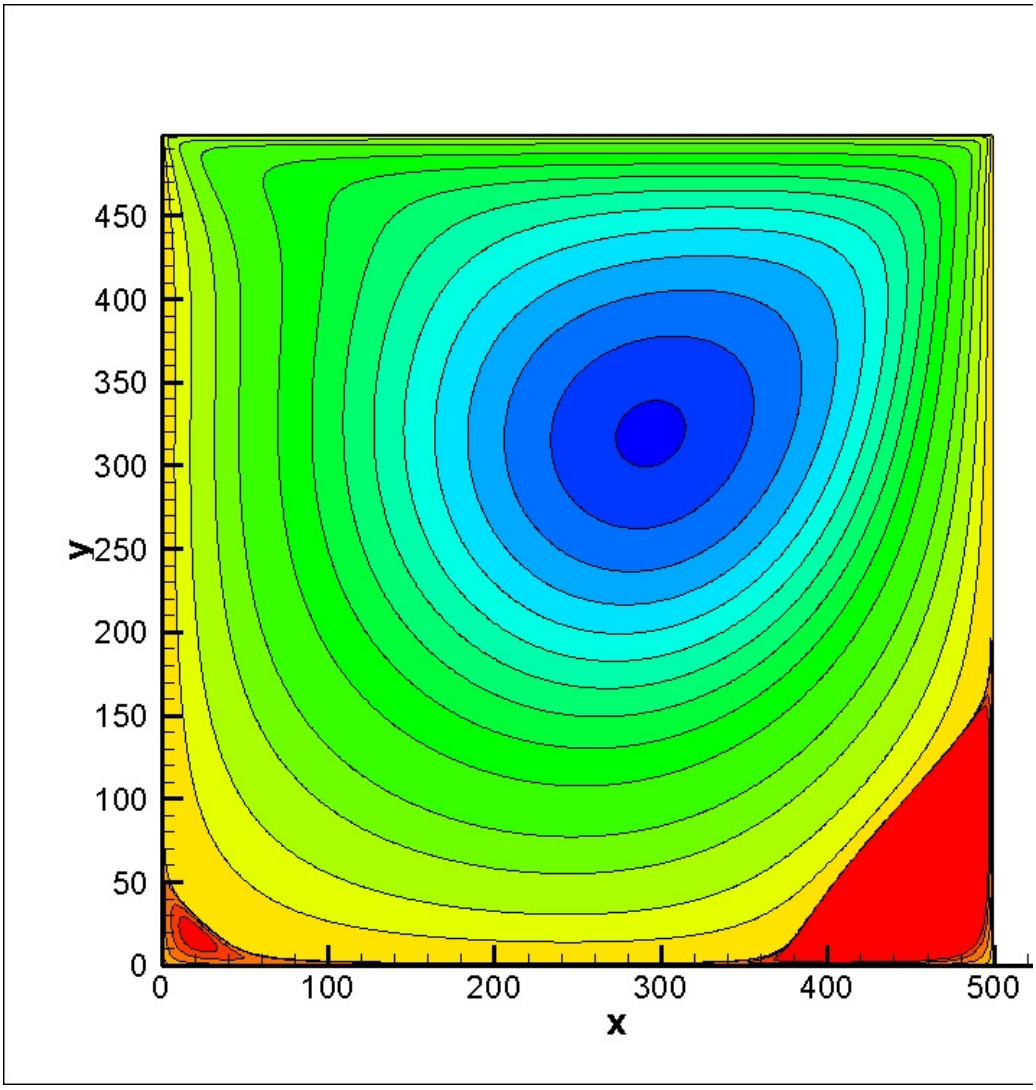


e) 500x500

Figure 4 Stream functions plotted for various grid resolutions: a) 50x50 , b) 100x100, c) 200x200, d) 300x300. Simulations are conducted for *Re*=300.

**c) Validation**

This method is validated by comparing its results with those obtained by Burggraf. Shown in figure 5 and figure 6 are the contours of the streamlines, result (a), and the contours of the vorticites, result (b). The results in figure 5 were obtained at a *Re* of 100 and the results in figure 6 were obtained at a *Re* of 400. These results are meant to be compared with those displayed in Burggraf's figure 9 [**Burggraf,1966**]. In the *Re*=100 case, the streamlines in both Burggraf's results and in the results obtained by this model show the formation of the corner vortices. As expected for a *Re* this low, both results display very small corner vortices. Also as expected, both results show that the corner vortex at the side which the lid is moving towards is larger. Possibility the best way to see the similarity is check the position of the center of the large recirculating region. The position of this flow structure depends heavily on *Re* and is therefore a good way to check these results. For the *Re*=400 case, the same comparisons need to be made. Again the location of the center of the large recirculating region is compared and both results agree very well. More impressive is the structure of the secondary vortices. Now that the secondary vortices are more defined, it has become more apparent that Burggraf's results are nearly identical to the results obtained by LBM. The next comparison to make is the votricity contours. Vorticity is a much harder flow property to compare. This is because it involves a derivative of velocity, any small errors in the velocity field will become exaggerated. Nevertheless, the vorticity contours for both *Re* agree reasonable well and depict the same overall structures.

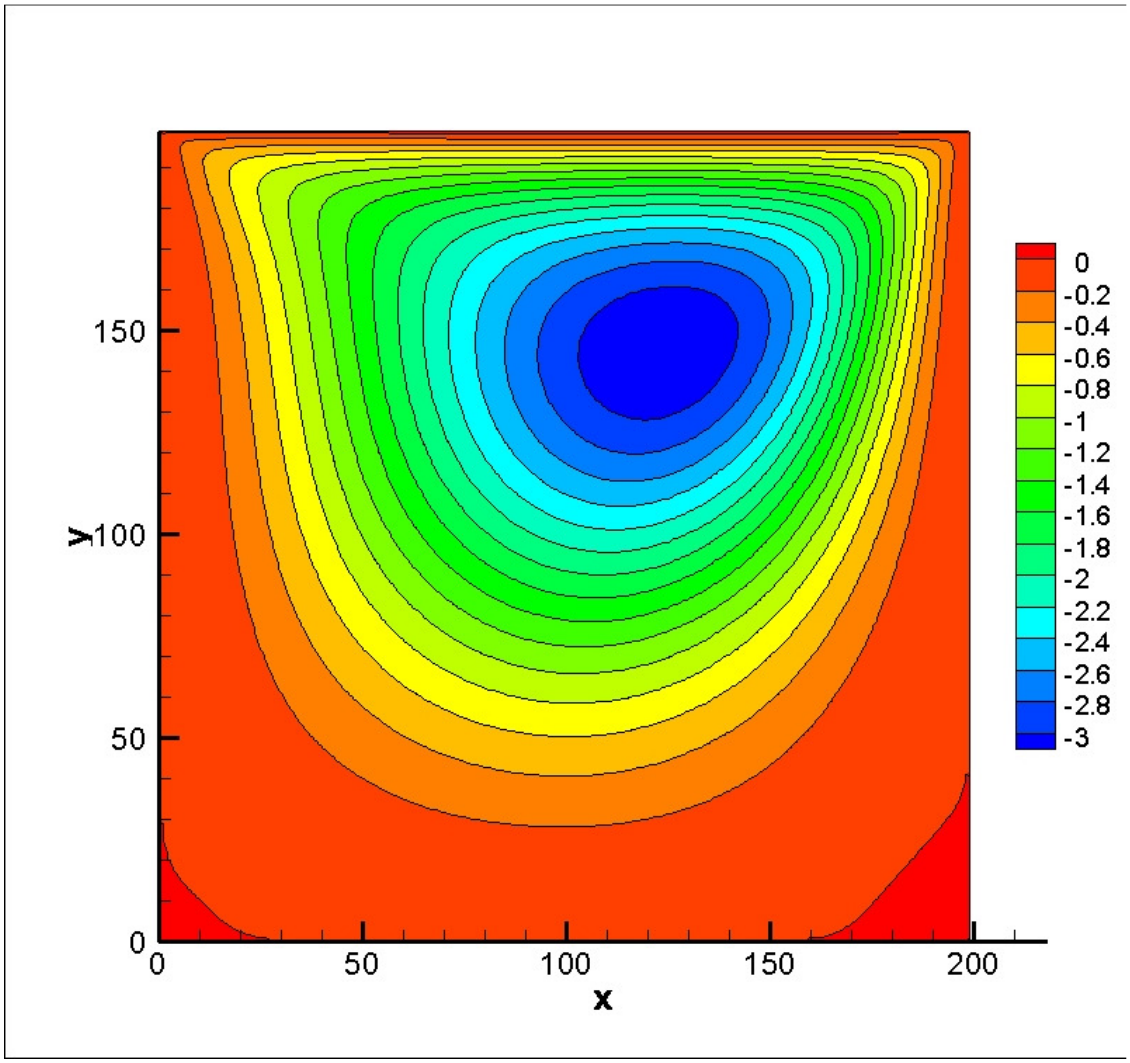


a) Stream function

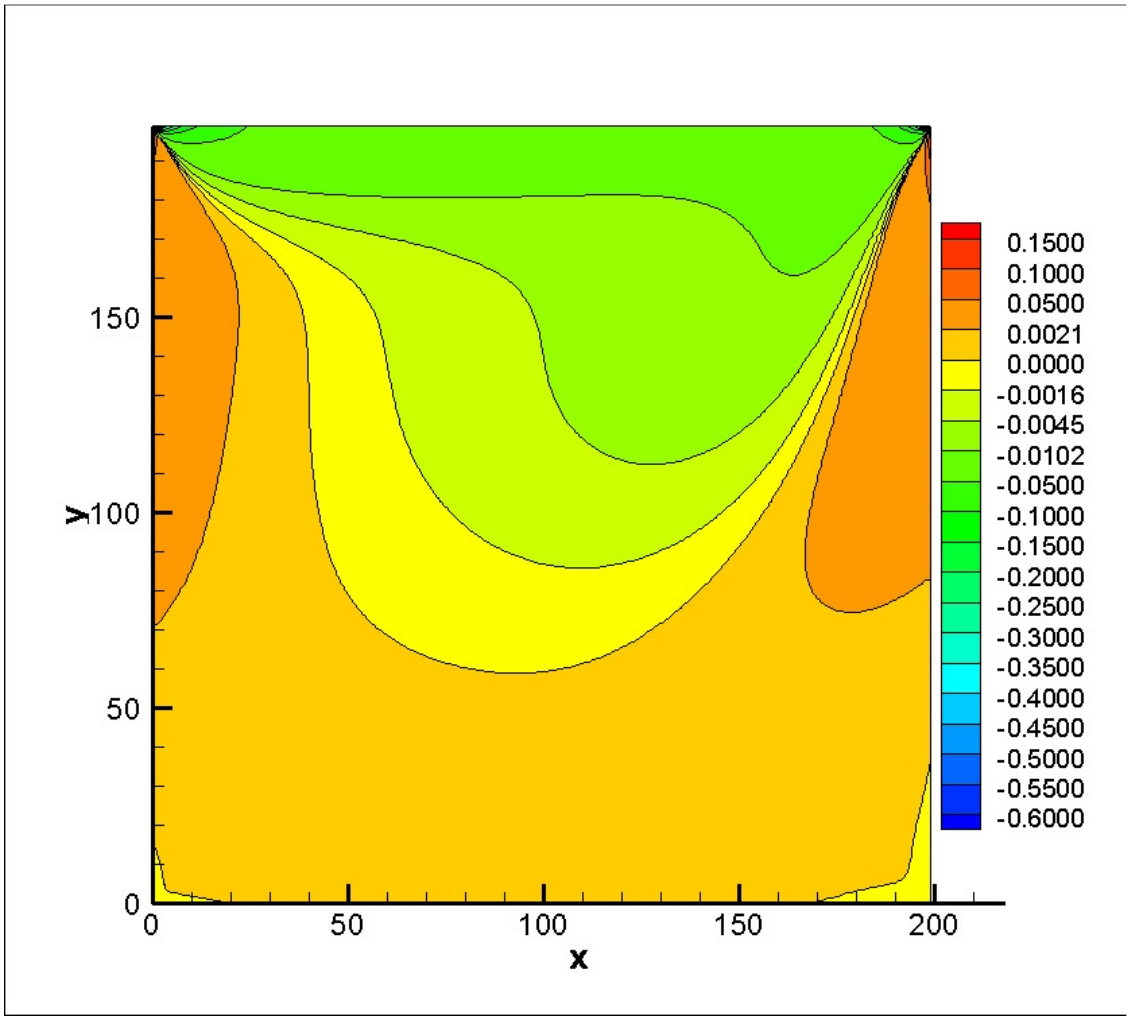


b) Vorticity

Figure 5 Stream function (a) and Vorticity (b) presented for *Re*=100 to be compared against Burggraf [**Burggraf,1966**]

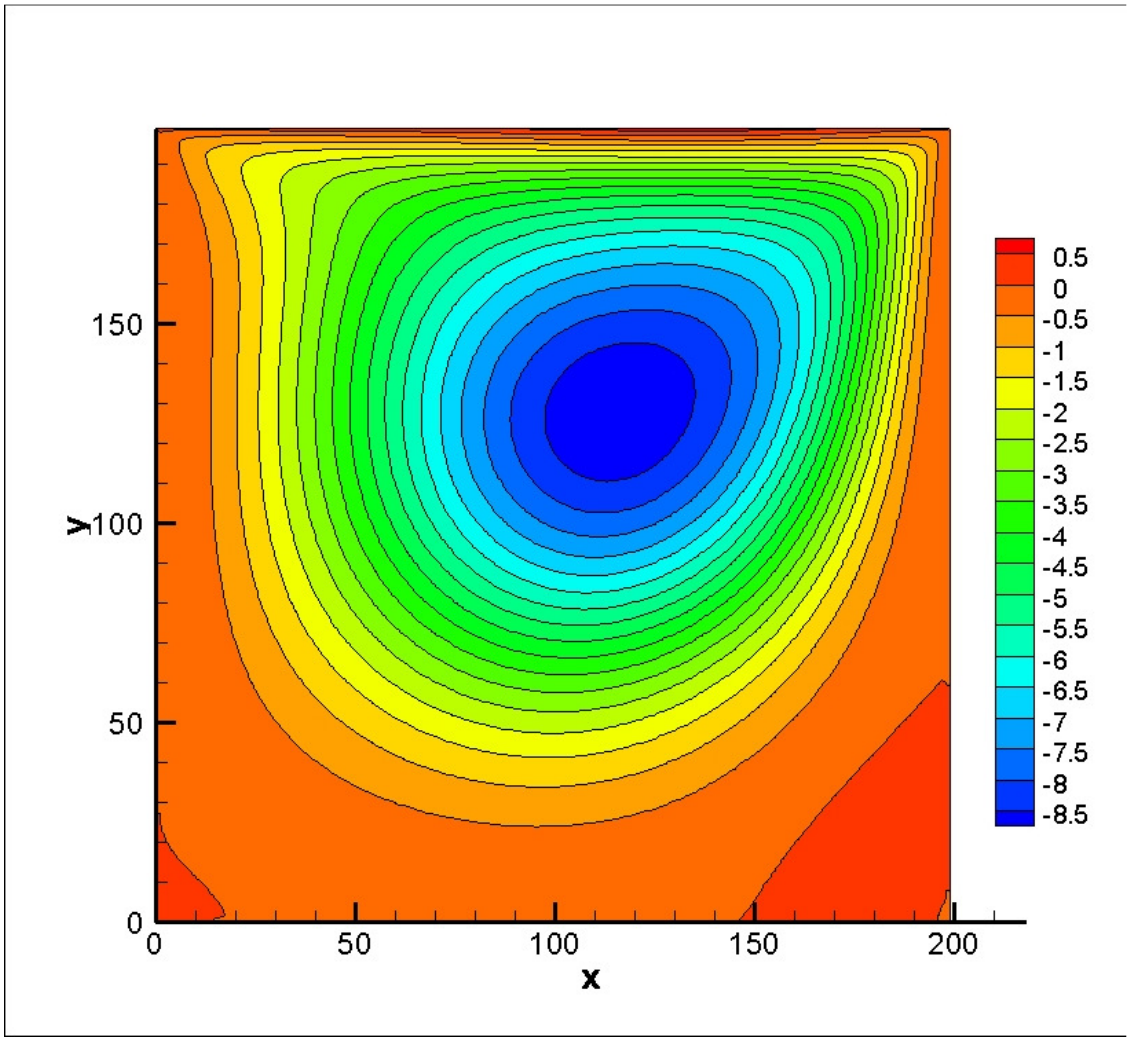


a) Stream function

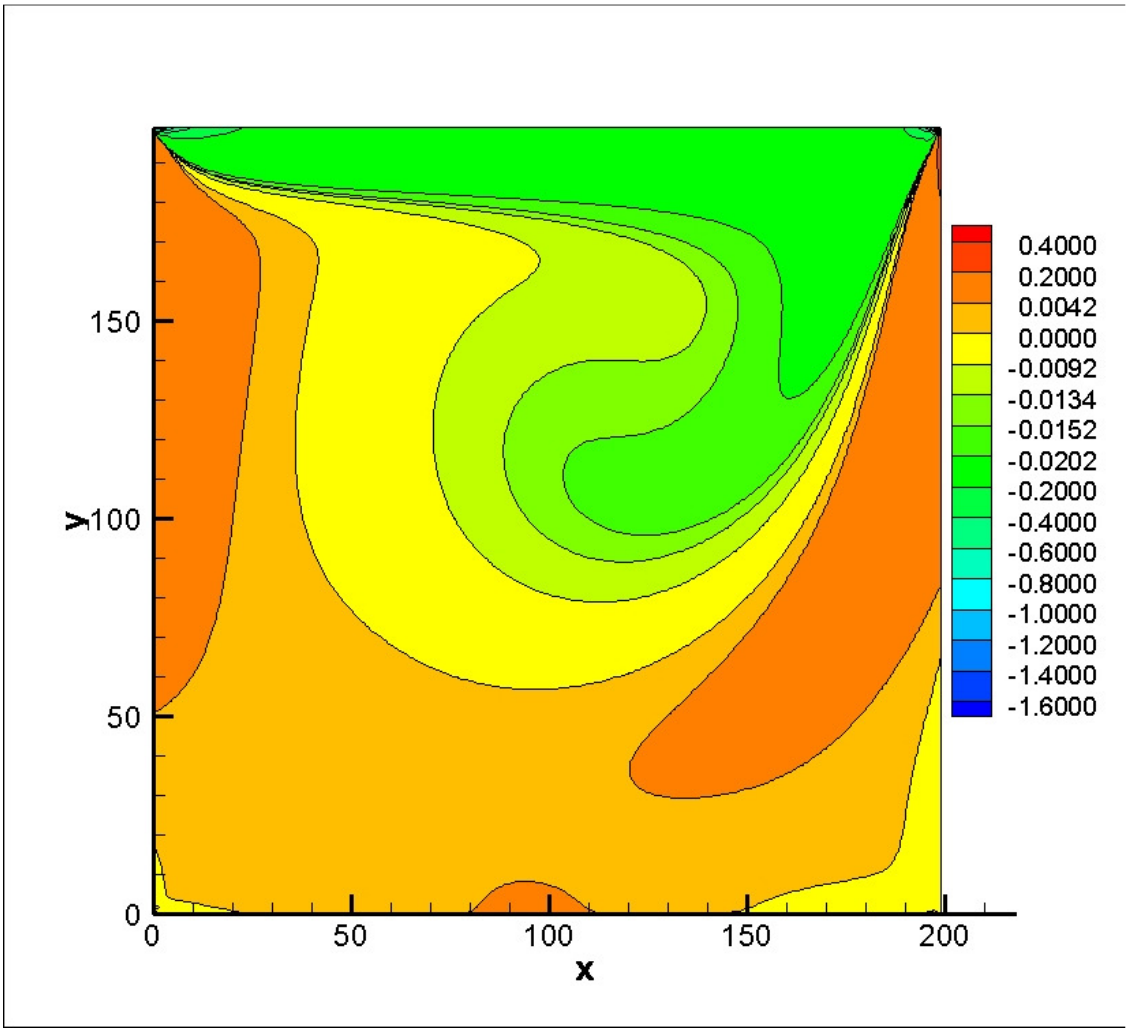


b) Vorticity

Figure 6 Stream function (a) and Vorticity (b) presented for *Re*=400 to be compared against Burggraf [**Burggraf,1966**]

**d) Entropic Method Results**

Presented in figure 7 are the contours of the streamlines (a) and the contours of the vorticity (b) for the case of *Re*=300. For comparison purposes the streamlines (c) and vorticity (d) are presented for the single relaxation time model using the same resolution. These results were obtained with the Entropic LBM variation. The result presented here was obtained with a fairly poor resolution, only a 100x100. Furthermore, the boundary treatment applied here causes stability problems at *Re* only slightly higher than what the standard LBM could do. Despite all these problems, this preliminary result can be compared to the single relaxation time results obtained above and serves the purpose of validating this method. As a future project, the present author will attempt to improve on these results so that this method can be used to study high *Re* flows.

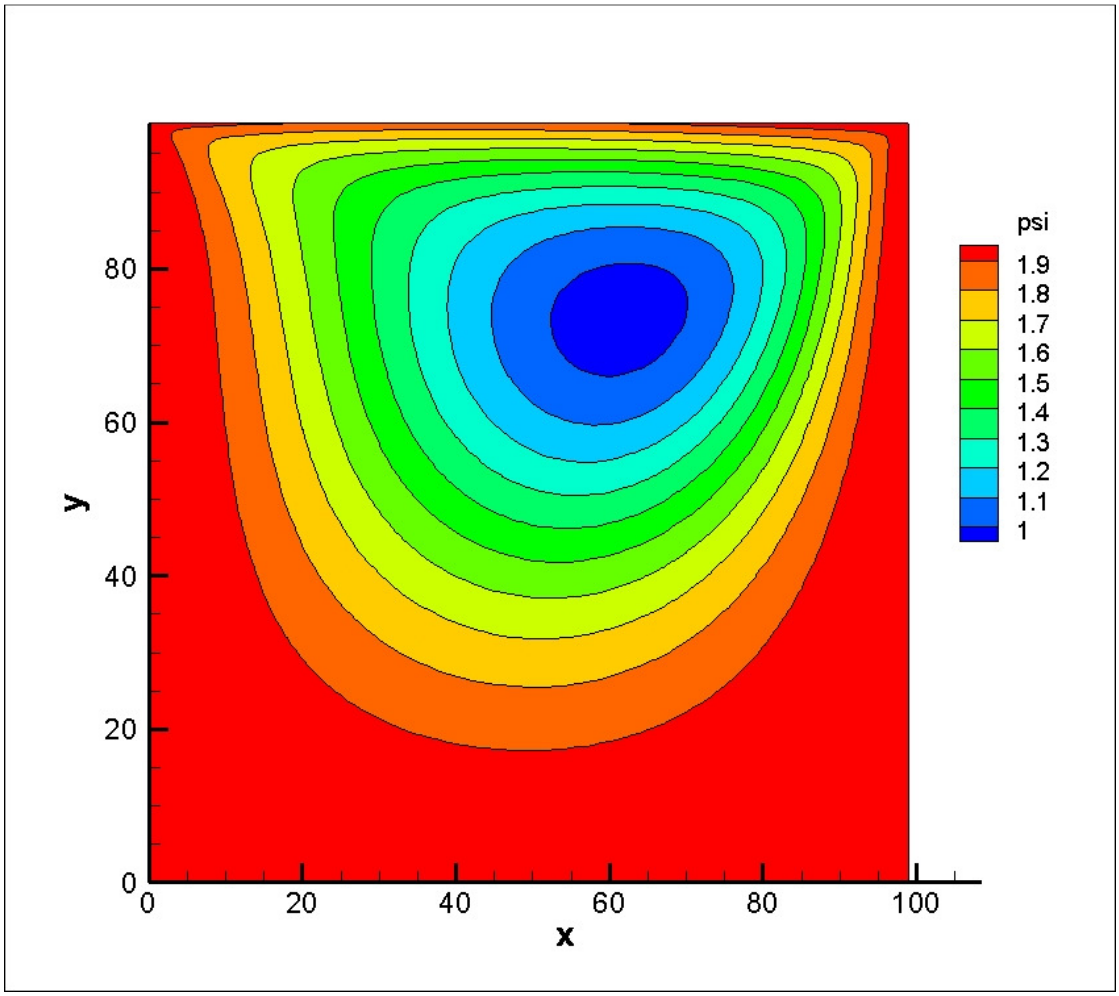


a) Stream function – Entropic LBM

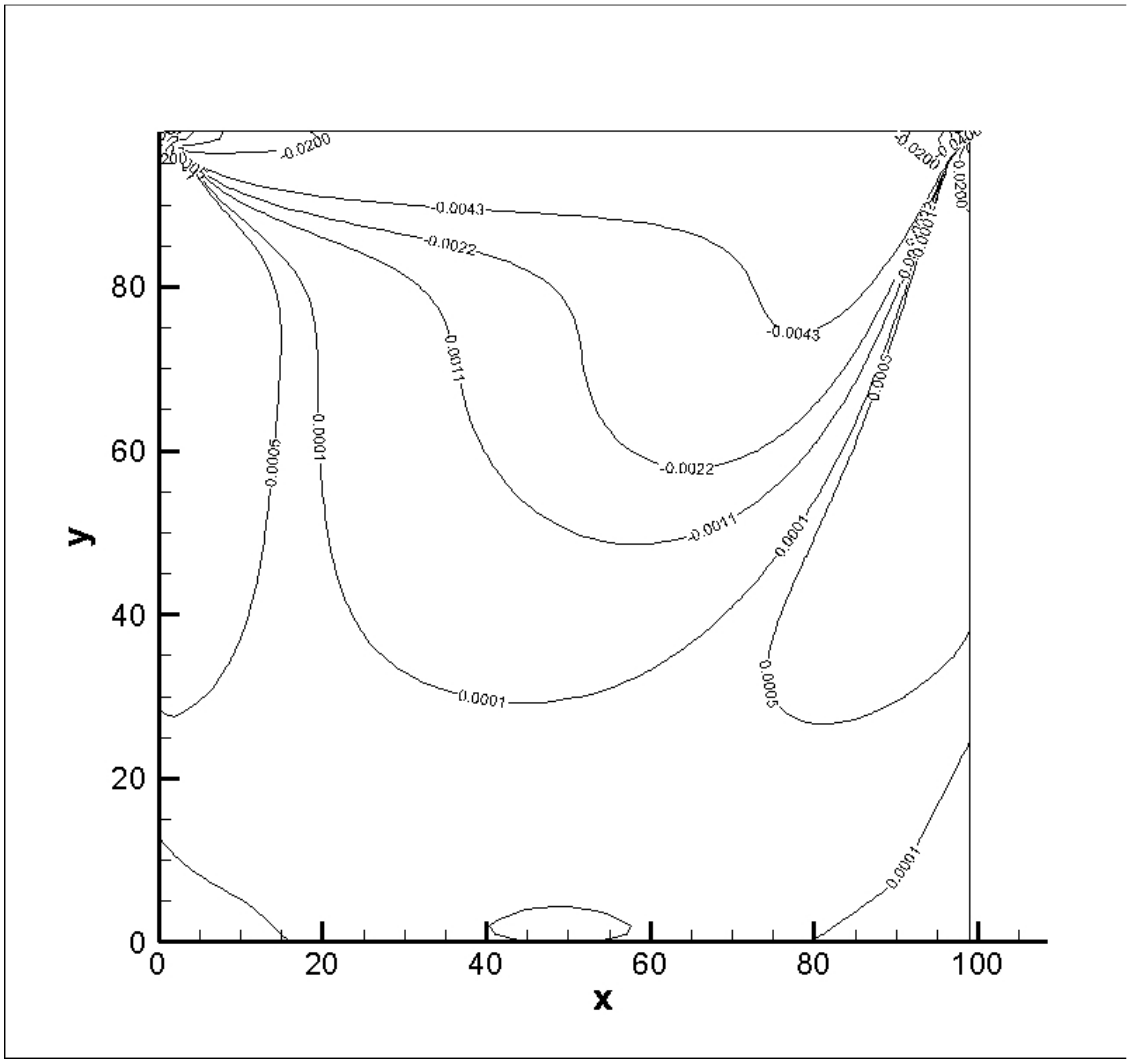


b) Vorticity – Entropic LBM

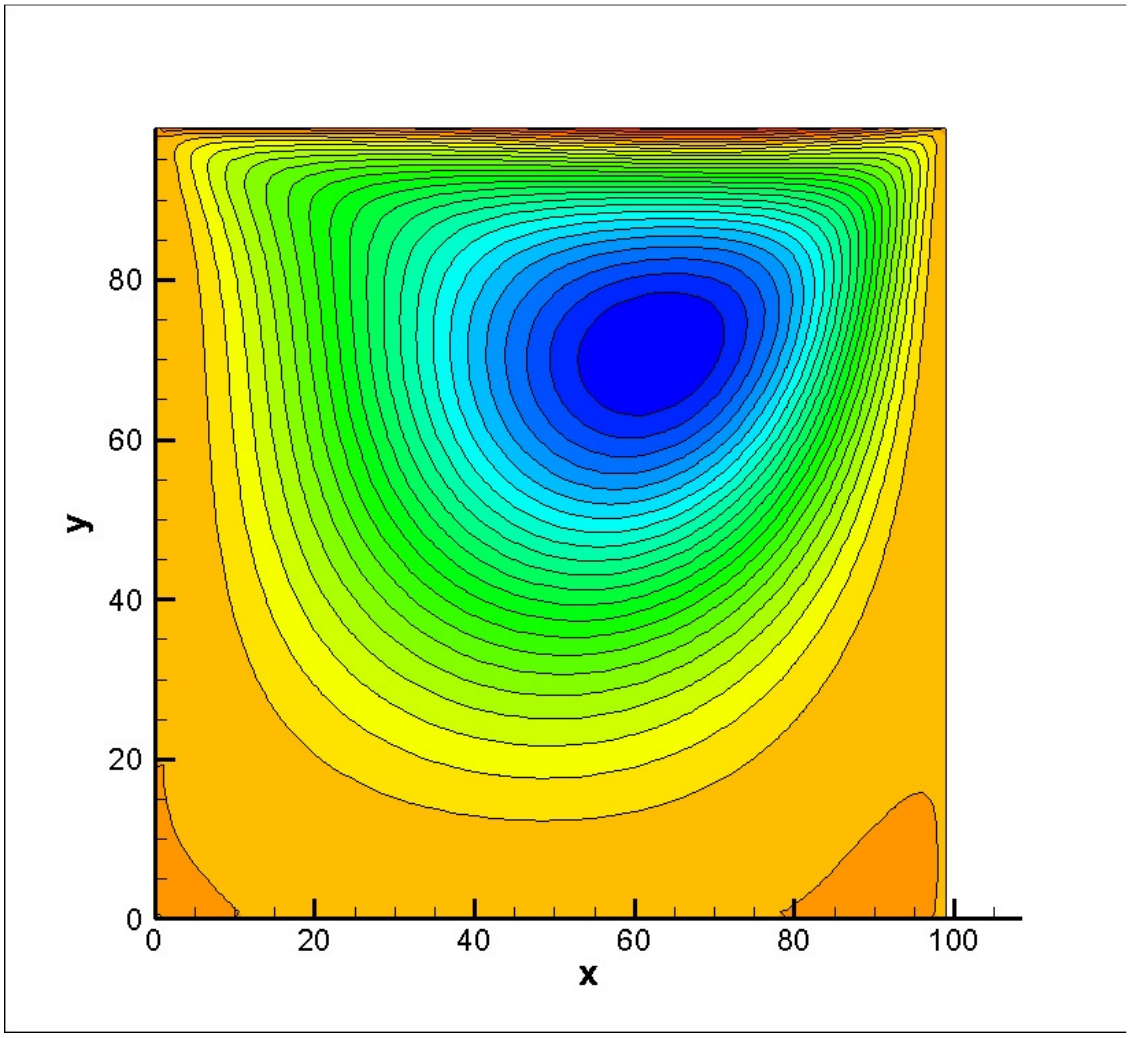


c) Stream function – Single Relaxation Time LBM

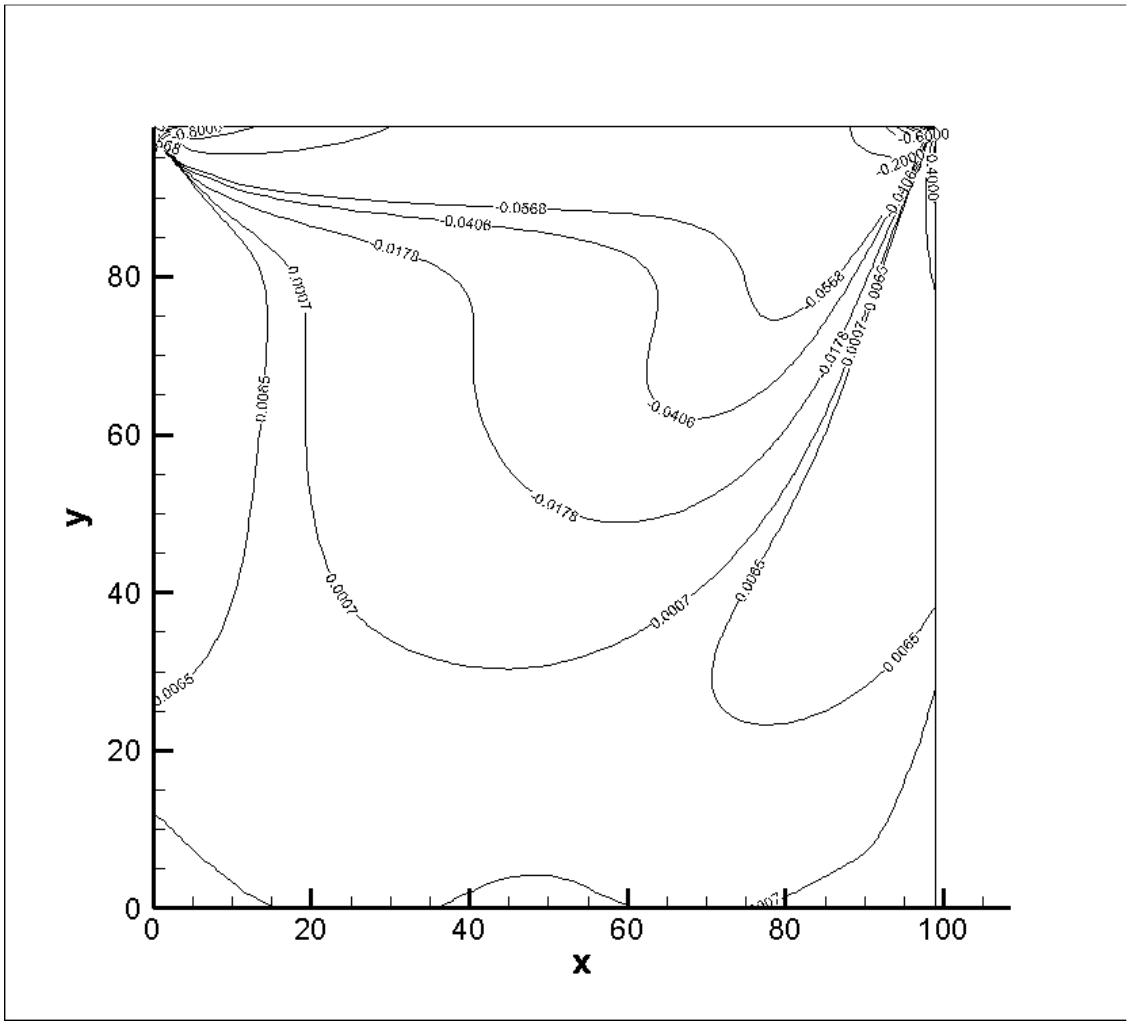


d) Vorticity – Single Relaxation Time LBM

Figure 7 Comparison between results obtained by Entropic LBM (a,b) and Single Relaxation Time LBM (c,d). Stream functions (a,c) and vorticity (b,d) are plotted for *Re*=300.

**e) Three Dimensional Results**

Figures 8 though 10 depict the lid-driven cavity problem in three dimensions. In this result the resolution is only 50x50x50, that is well below what is needed for convergence. As a result of this low resolution, the accuracy is not very high. Despite this, the classical flow structures can be seen. Away from the boundaries in the z direction, the flow resembles the two dimensional lid-driven cavity, as seen in figure 8 (c) and compared with figure 4. At the edges, secondary vortices are beginning to form, this can be seen in any of the images depicted in figure 8. Finally near the z directional walls, the boundary effects dampen the classical two dimensional lid-driven cavity flow structures, best seen in figure 8 (c). The corner vortices in the three dimensional lid-driven cavity flow appears to be smaller than its two dimensional counterpart. This could be attributed to real three dimensional effects. The y and z components of velocity depicted in figures 9 and 10 illustrate how complicated the flow structures becomes in three dimensions.

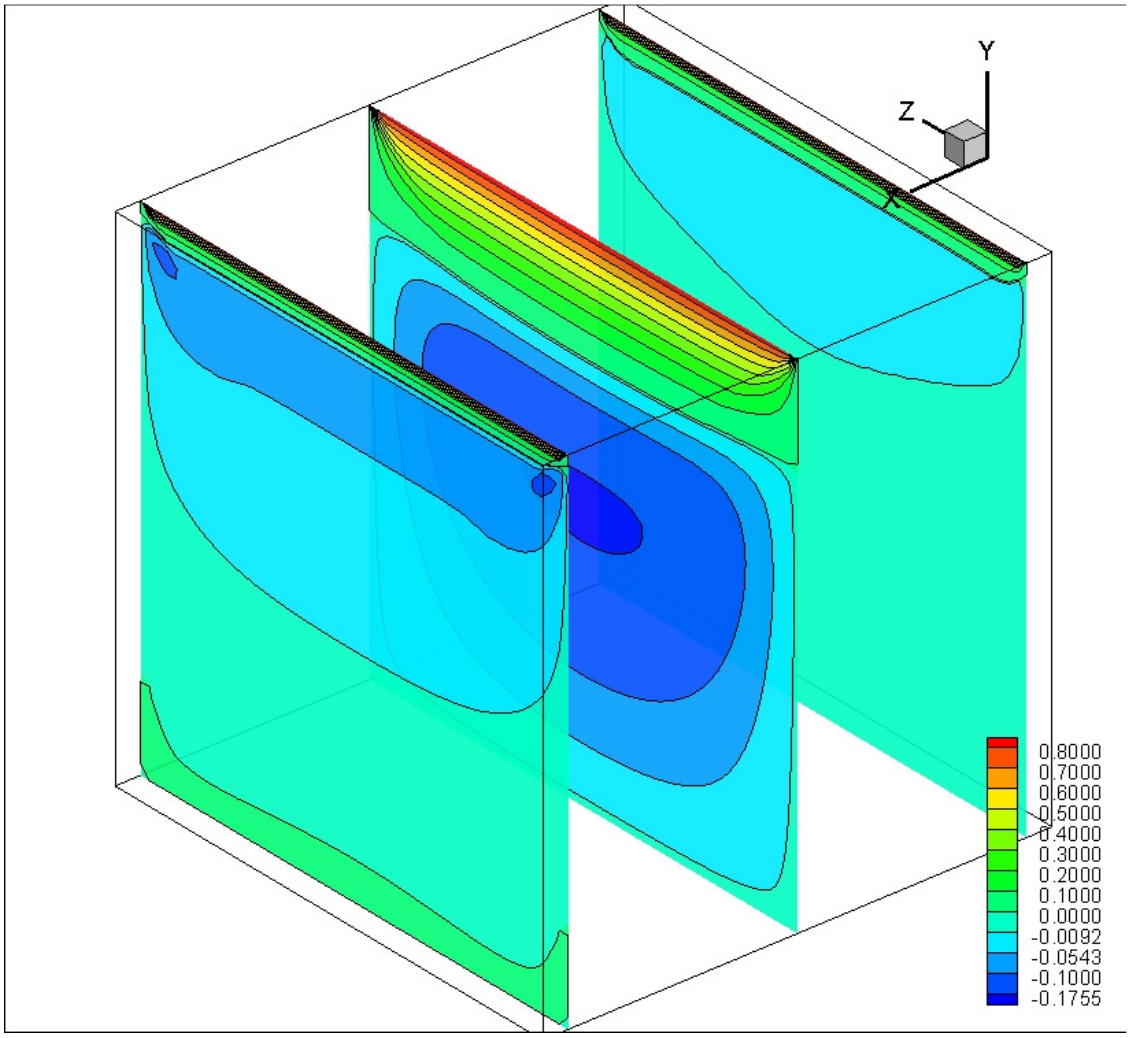


a) x component of velocity – cross sections on the x plane

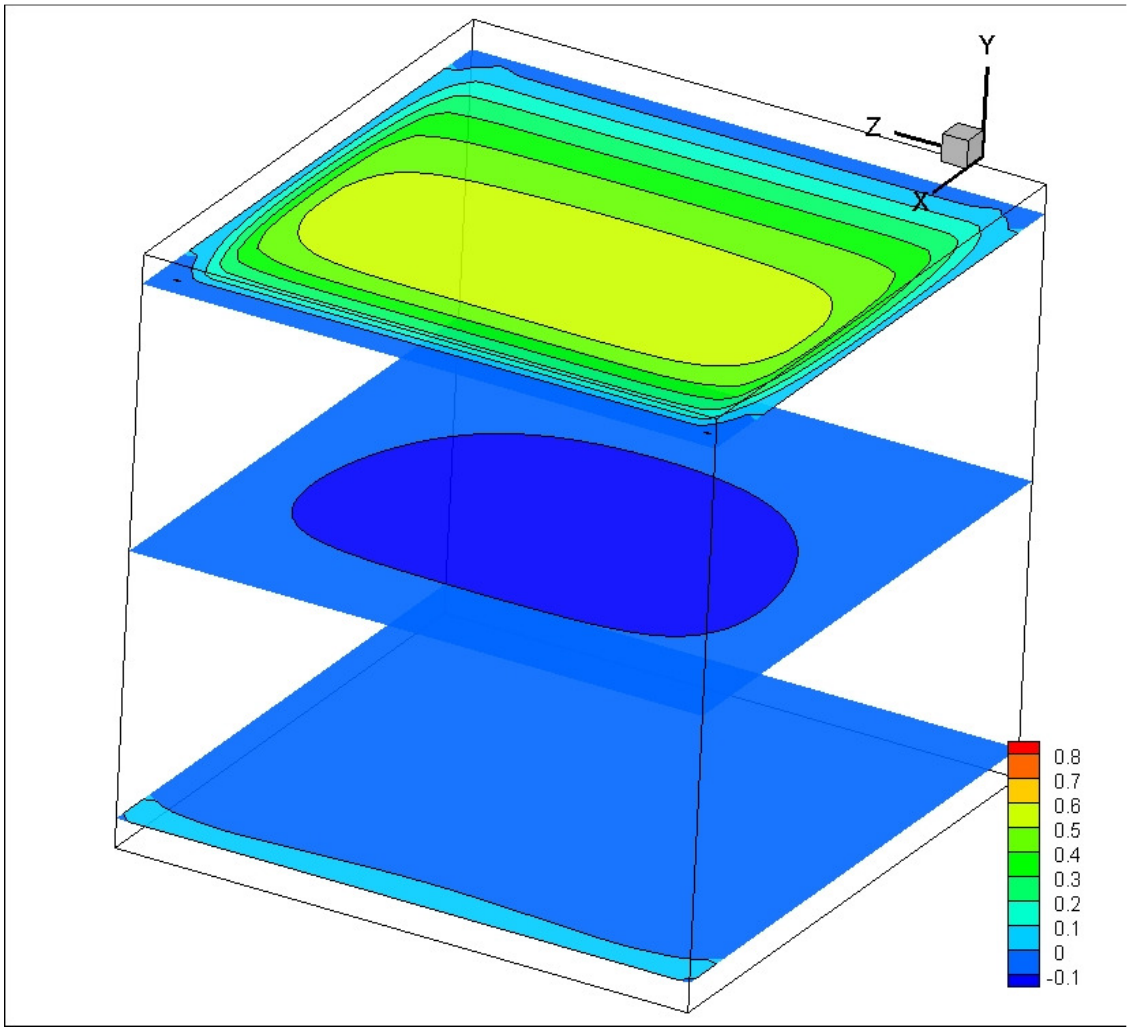


b) x component of velocity – cross sections on the y plane

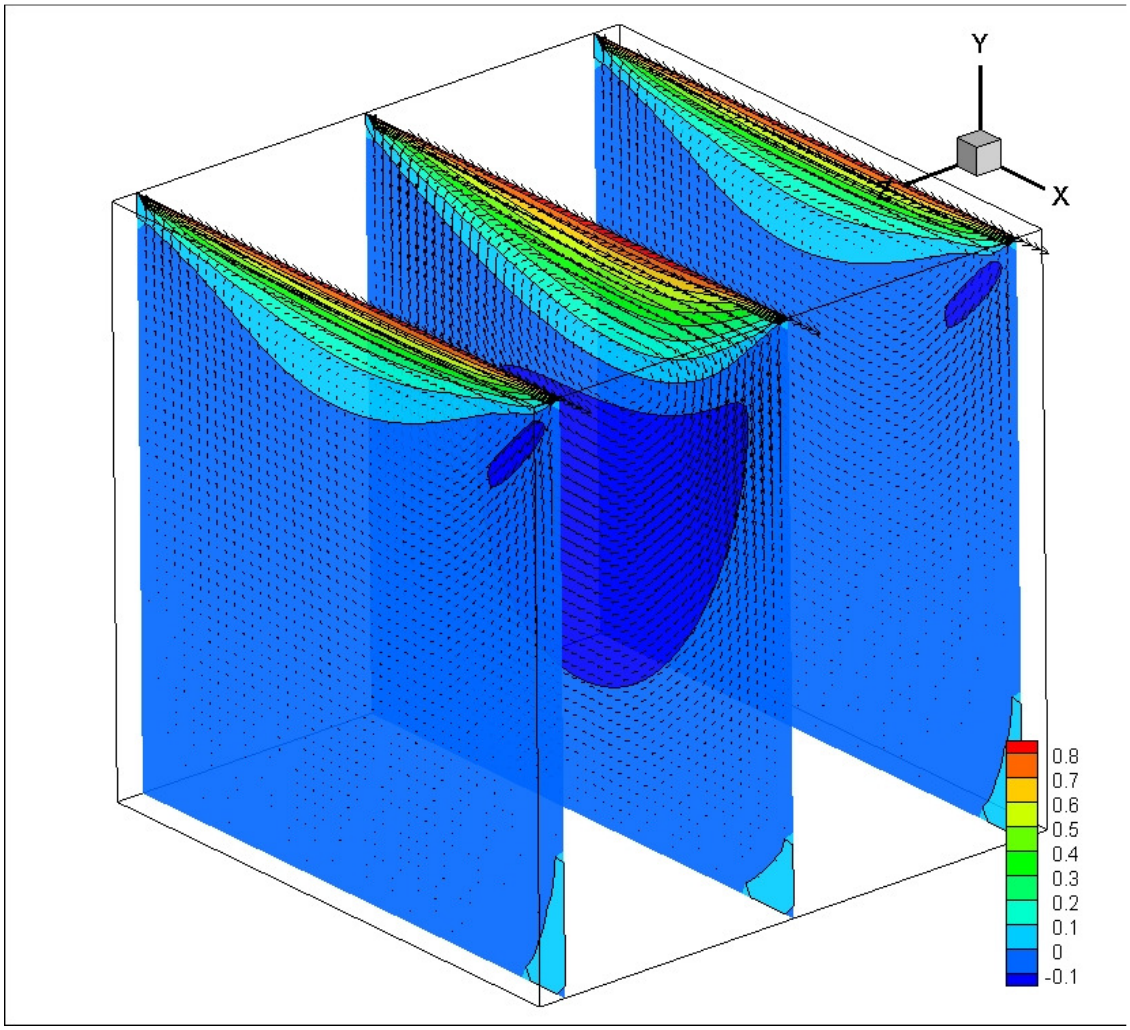


c) x component of velocity – cross sections on the z plane, velocity vectors are displayed

Figure 8 contours of the x component of velocity at a) the x plane, b) the y plane, and c) the z plane. Cross sections are presented at the center point and two nodes in from either boundary. Velocity vectors are displayed on the z plane.

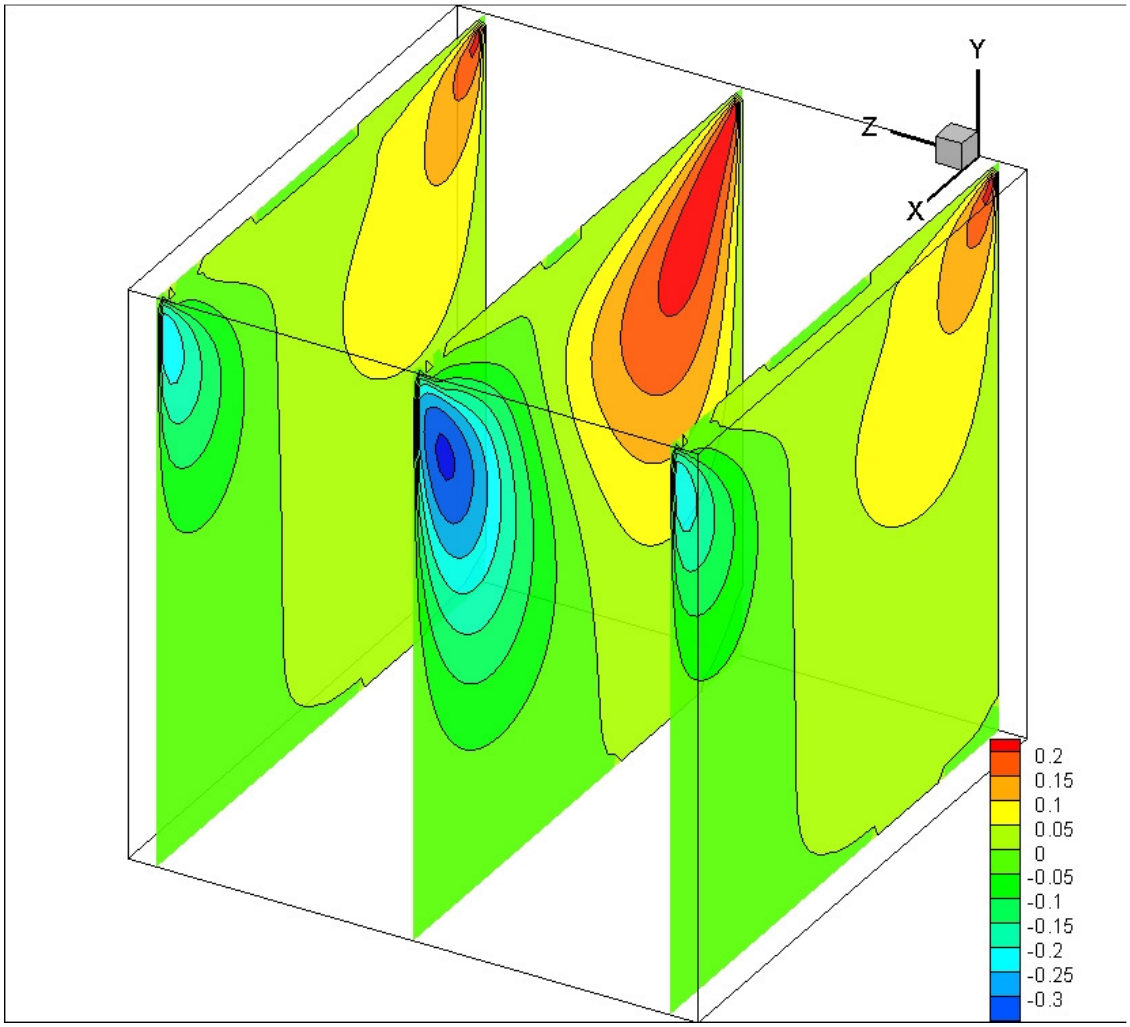


Figure 9 The contours of the y component of velocity displayed on cross sections of the z plane. Cross section are taken at the midpoint, and at two nodes in from either boundary.

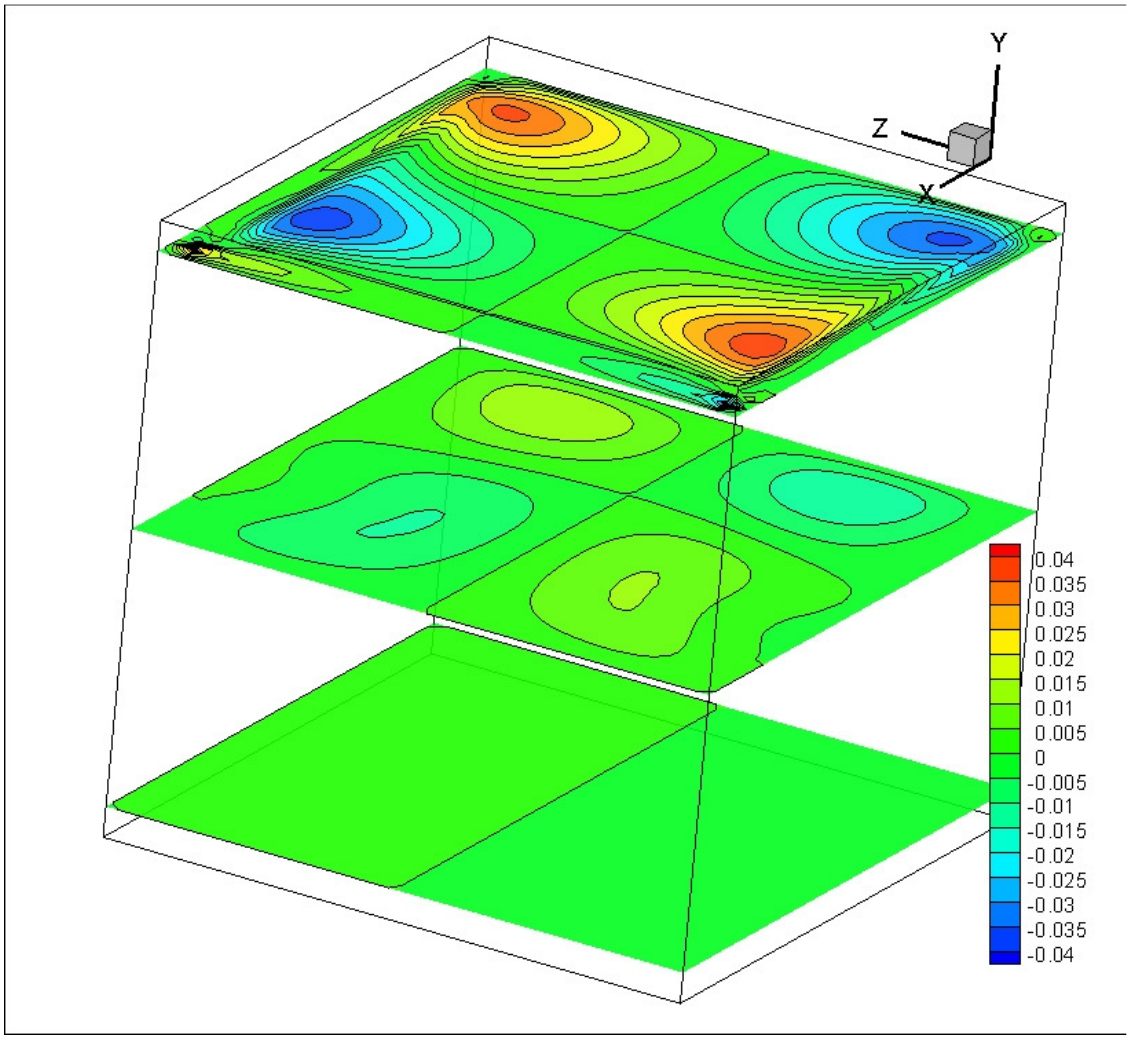


Figure 10 The contours of the z component of velcoty displaced at various cross sections on the z plane. The cross sections are taken at the midpoint and two nodes in from either boundary.

## 5. Conclusion

A detailed model of the single relaxation time Lattice Boltzmann Method is presented. In order to address the shortcomings of said model; the Regularized Lattice Boltzmann Method, the Multi-Relaxation Time Lattice Boltzmann Method, and the Entropic Lattice Boltzmann Method are presented. As an illustration, a lid driven cavity flow is studied with the single relaxation time Lattice Boltzmann Method and the Entropic Lattice Boltzmann Method in both two dimensions and in three dimensions for a Reynolds number of 300. The single relaxation time method, present with a very high resolution, is compared against previously reported results and agrees very well. Entropy method results are only preliminary and demonstrate that the method works. The resolution is low and more work is needed before entropy model can used to present accurate results. The results presented here demonstrate that Lattice Boltzmann can be easily extended to three dimensions. The three dimensional results are compared to the two dimensional results and it can be seen that far from the boundaries the same flow structure forms. It is shown that, even in the lid-driven cavity flow, three dimensional modeling produces complex flow patterns due to the boundary effects.

## 6. References


Aidun, Cyrus K., and Jonathan R. Clausen. "Lattice-Boltzmann Method for Complex Flows." *Annual Review of Fluid Mechanics* 42.1 (2010): 439-72. Web.

Almalowi, Saeed J., and Dennis E. Oztekin. "Nonlinear Dynamics of Rayleigh Taylor Instabilities Studied with a Lattice Boltzmann Method." *Journal of Mechanics Engineering and Automation* 4 (2014): 365-71. Print.

Almalowi, Saeed J., Dennis E. Oztekin, and Alparslan Oztekin, "Numerical Simulations of Lid-Driven Cavity Flows using Multi-relaxation Time Lattice Boltzmann Method" *Engineering Applications of Computational Fluid Dynamics (Advanced Structured Materials)* vol 44, edited by: Shaari, K., Zlati, K. and Mokhtar, A. Springer (Nov 2014).

Almalowi, Saeed J., Dennis E. Oztekin, and Alparslan Oztekin, "Regularized Multi-relaxation Lattice Boltzmann Method for Flow Past Square Cylinders", *Computers and Fluids*, 2013, (Under Review)

Bao, Jie, Peng Yuan, and Laura Schaefer. "A Mass Conserving Boundary Condition for the Lattice Boltzmann Equation Method." *Journal of Computational Physics* 227.18 (2008): 8472-487. Web.

Benzi, R., and S. Succi. "Two-dimensional Turbulence with the Lattice Boltzmann Equation." *Journal of Physics A: Mathematical and General* 23.1 (1990): L1-L5. Web.

Bhatnagar, P., E. Gross, and M. Krook. "A Model for Collision Processes in Gases. I. Small Amplitude Processes in Charged and Neutral One-Component Systems." *Physical Review* 94.3 (1954): 511-25. Web.

Boghosian, B. M., J. Yepez, P. V. Coveney, and A. Wager. "Entropic Lattice Boltzmann Methods." *Proceedings of the Royal Society A: Mathematical, Physical and Engineering Sciences* 457.2007 (2001): 717-66. Web.

Boghosian, Bruce, Peter Love, Peter Coveney, Iliya Karlin, Sauro Succi, and Jeffrey Yepez. "Galilean-invariant Lattice-Boltzmann Models with H Theorem." *Physical Review E* 68.2 (2003). Web.

Botella, O., and R. Peyret. "Benchmark Spectral Results on the Lid-driven Cavity Flow." *Computers & Fluids* 27.4 (1998): 421-33. Web.

Bouzidi, M'hamed, Dominique D'humières, Pierre Lallemand, and Li-Shi Luo. "Lattice Boltzmann Equation on a Two-Dimensional Rectangular Grid." *Journal of Computational Physics* 172.2 (2001): 704-17. Web.

Bruneau, Charles-Henri, and Mazen Saad. "The 2D Lid-driven Cavity Problem Revisited." *Computers & Fluids* 35.3 (2006): 326-48. Web.

Burggraf, Odus R. "Analytical and Numerical Studies of the Structure of Steady Separated Flows." *Journal of Fluid Mechanics* 24.01 (1966): 113. Web.

Chikatamarla, S. S., S. Ansumali, and I. V. Karlin. "Entropic Lattice Boltzmann Models for Hydrodynamics in Three Dimensions." *PHYSICAL REVIEW LETTERS* 97.1 (2006): 1-4. Web.

Chikatamarla, S.s., and I.v. Karlin. "Entropic Lattice Boltzmann Method for Turbulent Flow Simulations: Boundary Conditions." *Physica A: Statistical Mechanics and Its Applications* 392.9 (2013): 1925-930. Web.

D'humieres, D., I. Ginzburg, M. Krafczyk, P. Lallemand, and L.-S. Luo. "Multiple-relaxation-time Lattice Boltzmann Models in Three Dimensions." *Philosophical Transactions of*

*the Royal Society A: Mathematical, Physical and Engineering Sciences* 360.1792 (2002): 437-51. Web.

Frisch, U., B. Hasslacher, and Y. Pomeau. "Lattice-Gas Automata for the Navier-Stokes Equation." *Physical Review Letters* 56.14 (1986): 1505-508. Web.

Gunstensen, Andrew, Daniel Rothman, Stéphane Zaleski, and Gianluigi Zanetti. "Lattice Boltzmann Model of Immiscible Fluids." *Physical Review A* 43.8 (1991): 4320-327. Web.

Hardy, J., O. De Pazzis, and Y. Pomeau. "Molecular Dynamics of a Classical Lattice Gas: Transport Properties and Time Correlation Functions." *Physical Review A* 13.5 (1976): 1949-961. Web.

He, Xiaoyi, and Gary D. Doolen. "Thermodynamic Foundations of Kinetic Theory and Lattice Boltzmann Models for Multiphase Flows." *Journal of Statistical Physics* 107.1 (2002): 309-28. Web.

He, Xiaoyi, and Li-Shi Luo. "Lattice Boltzmann Model for the Incompressible Navier–Stokes Equation." *Journal of Statistical Physics* 88.3/4 (1997): 927-44. Web.

He, Xiaoyi, and Li-Shi Luo. "A Priori Derivation of the Lattice Boltzmann Equation." *Physical Review E* 55.6 (1997): R6333-6336. Web.

He, Xiaoyi, Shiyi Chen, and Gary D. Doolen. "A Novel Thermal Model for the Lattice Boltzmann Method in Incompressible Limit." *Journal of Computational Physics* 146.1 (1998): 282-300. Web.

He, Xiaoyi, Shiyi Chen, and Raoyang Zhang. "A Lattice Boltzmann Scheme for Incompressible Multiphase Flow and Its Application in Simulation of Rayleigh–Taylor Instability." *Journal of Computational Physics* 152.2 (1999): 642-63. Web.

Hou, Shuling, Xiaowen Shan, Qisu Zou, Gary D. Doolen, and Wendy E. Soll. "Evaluation of Two Lattice Boltzmann Models for Multiphase Flows." *Journal of Computational Physics* 138.2 (1997): 695-713. Web.

Huang, Haibo, Zhitao Li, Shuaishuai Liu, and Xi-Yun Lu. "Shan-and-Chen-type Multiphase Lattice Boltzmann Study of Viscous Coupling Effects for Two-phase Flow in Porous Media." *International Journal for Numerical Methods in Fluids* 61.3 (2009): 341-54. Web.

Házi, G., and C. Jiménez. "Simulation of Two-dimensional Decaying Turbulence Using the "incompressible" Extensions of the Lattice Boltzmann Method." *Computers & Fluids* 35.3 (2006): 280-303. Web.

Izham, Muhammad, Tomohiro Fukui, and Koji Morinishi. "Application of Regularized Lattice Boltzmann Method for Incompressible Flow Simulation at High Reynolds Number and Flow with Curved Boundary." *Journal of Fluid Science and Technology* 6.6 (2011): 812-22. Web.

Karlin, I. V., A. Ferrante, and H. C. Öttinger. "Perfect Entropy Functions of the Lattice Boltzmann Method." *Europhysics Letters (EPL)* 47.2 (1999): 182-88. Web.

Karlin, Iliya, and S. Succi. "Equilibria for Discrete Kinetic Equations." *Physical Review E* 58.4 (1998): R4053-4056. Web.

Keating, Brian, George Vahala, Jeffrey Yepez, Min Soe, and Linda Vahala. "Entropic Lattice Boltzmann Representations Required to Recover Navier-Stokes Flows." *Physical Review E* 75.3 (2007). Web.

Latt, Jonas, and Bastien Chopard. "Lattice Boltzmann Method with Regularized Pre-collision Distribution Functions." *Mathematics and Computers in Simulation* 72.2-6 (2006): 165-68. Web.

Liu, Chih-Hao, Kuen-Hau Lin, Hao-Chueh Mai, and Chao-An Lin. "Thermal Boundary Conditions for Thermal Lattice Boltzmann Simulations." *Computers & Mathematics with Applications* 59.7 (2010): 2178-193. Web.

Llewellin, E.w. "LBflow: An Extensible Lattice Boltzmann Framework for the Simulation of Geophysical Flows. Part I: Theory and Implementation." *Computers & Geosciences* 36.2 (2010): 115-22. Web.

Maier, Robert S., Robert S. Bernard, and Daryl W. Grunau. "Boundary Conditions for the Lattice Boltzmann Method." *Physics of Fluids* 8.7 (1996): 1788. Web.

Martínez, D. O., W. H. Matthaeus, S. Chen, and D. C. Montgomery. "Comparison of Spectral Method and Lattice Boltzmann Simulations of Two-dimensional Hydrodynamics." *Physics of Fluids* 6.3 (1994): 1285. Web.

Mei, Renwei, Wei Shyy, Dazhi Yu, and Li-Shi Luo. "Lattice Boltzmann Method for 3-D Flows with Curved Boundary." *Journal of Computational Physics* 161.2 (2000): 680-99. Web.

Mohamad, A.a., and A. Kuzmin. "A Critical Evaluation of Force Term in Lattice Boltzmann Method, Natural Convection Problem." *International Journal of Heat and Mass Transfer* 53.5-6 (2010): 990-96. Web.

Rothman, Daniel, and Stéphane Zaleski. "Lattice-gas Models of Phase Separation: Interfaces, Phase Transitions, and Multiphase Flow." *Reviews of Modern Physics* 66.4 (1994): 1417-479. Web.

Shan, Xiaowen, and Hudong Chen. "Lattice Boltzmann Model for Simulating Flows with Multiple Phases and Components." *Physical Review E* 47.3 (1993): 1815-819. Web.

Succi, S. *The Lattice Boltzmann Equation for Fluid Dynamics and beyond*. Oxford: Clarendon, 2001. Print.

Succi, Sauro, Roberto Benzi, and Francisco Higuera. "The Lattice Boltzmann Equation: A New Tool for Computational Fluid-dynamics." *Physica D: Nonlinear Phenomena* 47.1-2 (1991): 219-30. Web.

Swift, Michael, W. Osborn, and J. Yeomans. "Lattice Boltzmann Simulation of Nonideal Fluids." *Physical Review Letters* 75.5 (1995): 830-33. Web.

Yasduda, Takahiro, Tomohisa Hashimoto, Hisato Minagawa, Koji Morinishi, and Nobuyuki Satofuka. "Efficient Simulation for Incompressible Turbulent Flow Using Lattice Boltzmann Model." *Procedia Engineering* 61 (2013): 173-78. Web.

Yasuda, T., and N. Satofuka. "An Improved Entropic Lattice Boltzmann Model for Parallel Computation." *Computers & Fluids* 45.1 (2011): 187-90. Web.

Zou, Qisu, and Xiaoyi He. "On Pressure and Velocity Boundary Conditions for the Lattice Boltzmann BGK Model." *Physics of Fluids* 9.6 (1997): 1591. Web.

## 7. Vita

Dennis E. Oztekin was born in Champaign, Illinois in 1990. He is the son of Alparslan Oztekin and Hulya Akman Oztekin. Dennis Oztekin completed high school in 2009 at the Parkland school district. He then enrolled in Lehigh University for his undergraduate degree. At Lehigh Dennis completed pursued both a Bachelor of Science in Mathematics and a degree Bachelor of Science in Mechanical Engineering. After completing both degree in the summer semester of 2012, Dennis began pursuing his Master of Science in Mechanical Engineering with the intention of specializing in Fluid Mechanics. During his graduate work, Dennis began to get involved in kinetic theory and has since worked with the Lattice Boltzmann method. During his time as a graduate student at Lehigh University Dennis wrote a number of publications. He currently has one journal paper in print, one book chapter in print, five conference proceedings in print, and four more journal papers under review.